FINAL REPORT

National Water Research Institute

Development and Testing of New Nanofiltration Membranes for Application to Water Treatment: An Integrated Polymer Chemistry/Engineering Approach

Francis A. DiGiano, Principal Investigator
Denis Leroux, Post-Doctoral Research Associate
Anna Roudman, Post-Doctoral Research Associate
Dept. of Environmental Sciences and Engineering
University of North Carolina
Chapel Hill, NC 27599-7400

Benny D. Freeman, Co-Principal Investigator
Michelle Arnold, Graduate Research Assistant
Kazukiyo Nagai, Post-doctoral Research Associate
Dept. of Chemical Engineering
North Carolina State University
Raleigh, NC 27695-7905

Joseph M. DeSimone, Co-Principal Investigator
Douglas Betts, Graduate Research Assistant
Terri Johnson, Graduate Research Assistant
Dept. of Chemistry
University of North Carolina
Chapel Hill, NC 27599-3290

July 1, 1999

Table of Contents

Acknowledgments

Some of the results presented herein were obtained with research grants from the Office of Naval Research and the American Water Works Research Foundation either concurrently with this project or immediately following its termination.

Introduction

Minimizing the frequency with which membranes must be rinsed and/or cleaned to remove foulant materials is essential before membrane separation is accepted as a "conventional" water treatment process. Most studies to date compare the performance of commercially available membranes at a particular site and thus have not linked materials science and process engineering in a way to improve membrane technology for drinking water and particularly for removal of natural organic matter (NOM), the precursor to regulated disinfection by-products. This research forged the disciplines of environmental engineering, chemical engineering, and polymer chemistry in order to explore new membrane materials and ultimately to develop high performance, ultralow fouling membrane materials.

Several new block copolymer formulations were synthesized and characterized in this research. Two were prepared as thin-film composite membranes with a polysulfone support layer in order to compare their water permeation, NOM rejection, and fouling properties commercial nanofiltration membrane. The ultimate goal was to produce a nanofiltration membrane that can reject NOM as effectively as commercially available membranes but with either less tendency for fouling or easier cleaning ability. This report includes highlights of the results from synthesis and characterization of block copolymers, testing of the dense film properties of these materials, and testing of two, thin-film composite membranes with a water obtained from a water treatment plant in NC.

Research Team Organization

The research team organization and responsibilities are shown in Figure 1. The research was collaborative with Dr. J. DeSimone of the Department of Chemistry at the University of North Carolina/Chapel Hill (UNC) who led the synthesis effort and with Dr. B. Freeman of the Department of Chemical Engineering at North Carolina State University (NCSU) who led the effort in dense film preparation and characterization prior to the production of thin-film composite membranes.

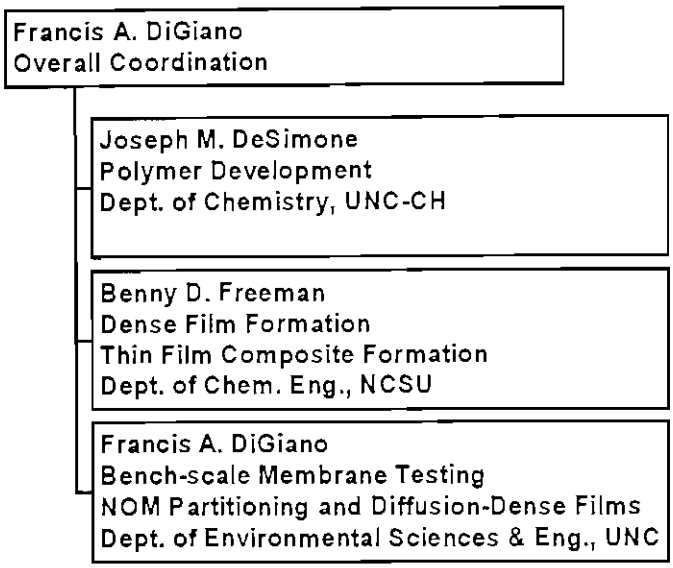

Figure 1. Organization and Responsibilities of Research Team Members

Block Copolymers

The focus of the synthesis work was on *block* copolymers. These are formed by covalent chemical linking of two monomers, M_1 and M_2, in a repeating pattern. For instance, a diblock copolymer has the repeating formulation M_1-b-M_2. Block copolymers can *microphase segregate* to form channels, such as shown in Figure 2, or other domains. By contrast, the monomer units are linked randomly in *random copolymers*, which prevents the formation of a segregated phase. In Figure 2, the fluorocarbon segment provides a minimally adhesive veneer which could reduce membrane fouling and/or improve membrane cleaning efficiency. The hydrophilic segments self-assemble to form hydrophilic channels or "highways" for high rates of water permeation. These channels represent the molecular space occupied by the hydrophilic polymer and should not to be confused with pores as, for example, in ultrafiltration membranes. The "diameter" of the channels is on the order of nanometers.

To produce a *thin-film composite membrane,* a block copolymer is cast as a thin-layer on a microporous support. The *microphase-separated block copolymers* that were synthesized in this research have not been previously investigated for use as membrane materials.

Figure 2. General Features of Block Copolymers For Formulation Into Nanofiltration Membranes

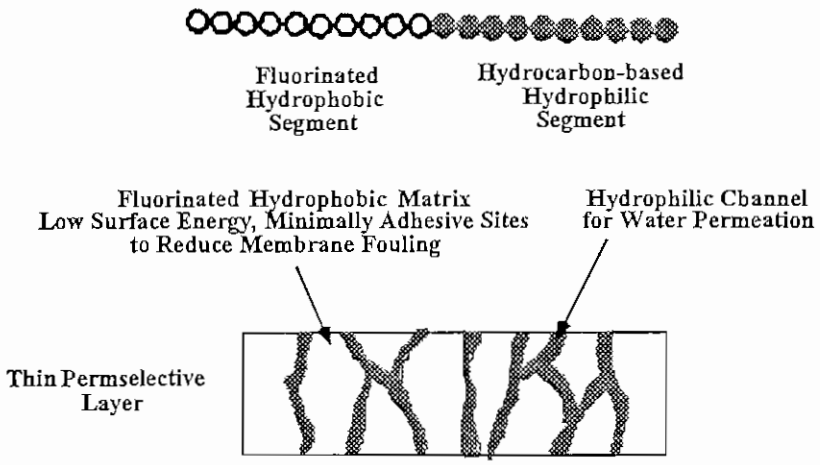

Several different hydrophilic domains were embedded into a very low surface energy (<11 dynes cm^{-1}) fluorocarbon matrix derived from poly(*n*-fluoroalkyl acrylate and methacrylate)-based block copolymers. In particular, poly(1,1-dihydroperfluoro-octyl acrylate) [poly(FOA)] has an extraordinarily low surface free energy, reported to be < 11 dynes cm^{-1}, [1,2] which is much lower than poly(dimethylsiloxane) (22 dynes cm^{-1}) [3], poly(tetrafluoroethylene) (18.7 dynes cm^{-1}), and poly(hexafluoropropylene) (16.7 dynes cm^{-1}). This class of materials has, therefore, the distinction of being the *lowest surface free energy polymeric materials known*. As a result, these novel materials, when used as the permselective barrier layer in composite membranes, should exhibit low adhesive energy.

Fluoropolymer-based permselective barrier layers for composite membranes should offer significant advantages over conventional systems, especially related to fouling, because of their very low surface free energy and the ability to use compositional and architectural control to tailor physical characteristics. Of the research in the last 40 years on block and graft copolymers, fluorinated materials have received very little attention. This trend, however, is not based on a perception that the materials would not be very interesting. In fact, quite to the contrary, the materials have enjoyed considerable

speculation regarding their utilization in many diverse applications. The problem lies in their synthesis—the synthesis of fluoropolymers has traditionally been difficult due to their inherent insolubility—recently Professor DeSimone's laboratory has addressed this synthetic problem.

Professor DeSimone and coworkers have reported[4] the successful synthesis of high molar mass fluoropolymers using homogeneous free radical solution polymerization methods in supercritical carbon dioxide as shown in Figure 3. These fluoropolymers, based on the polymerization of 1,1-dihydroperfluorooctyl acrylate (FOA), are used commercially as protective coatings in many diverse applications because they are generally insoluble in many traditional organic solvents—the only known solvents are chlorofluorocarbons (CFCs).

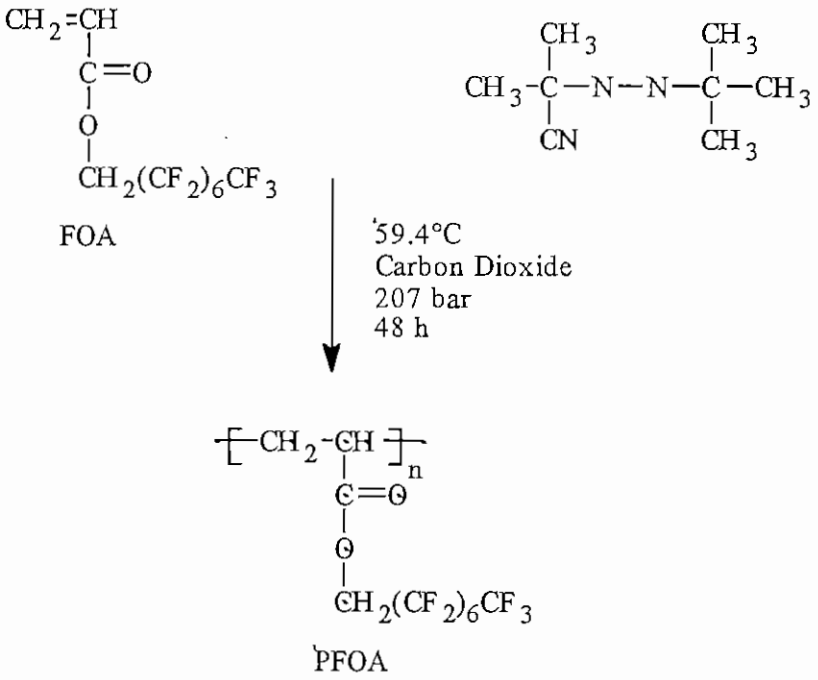

Figure 3. Polymerization of Ultralow Surface Energy Polymers in Supercritical CO_2

The synthesis of fluoropolymers in CO_2 not only offers an environmentally sound solvent choice but offers much more in being able to synthesize new fluoropolymers that are not synthetically accessible using conventional solvents.[5-8] This is a direct result of conducting polymerizations in carbon dioxide homogeneous, one phase reactions (for the

synthesis of copolymers and functionalized polymers) having an inherently low solution viscosity (no Tromsdorff effects giving clean molar mass distributions) under inert conditions (no detectable chain transfer to solvent). Using a combination of methods, Professor DeSimone's team was able in this research to synthesize microphase-separated fluoropolymers having hydrophilic dispersed phases.

Overview of Research Tasks

The research tasks related to polymer synthesis and characterization and dense film testing are described in Figure 4. Results of structure-activity relationships of block copolymer formulations were obtained from Dr. Harry Ridgway of the Orange County Water District of Southern California. However, these will not be discussed because the data were limited. Such studies would be beneficial in follow-up research that continues to relate polymer chemistry to membrane performance.

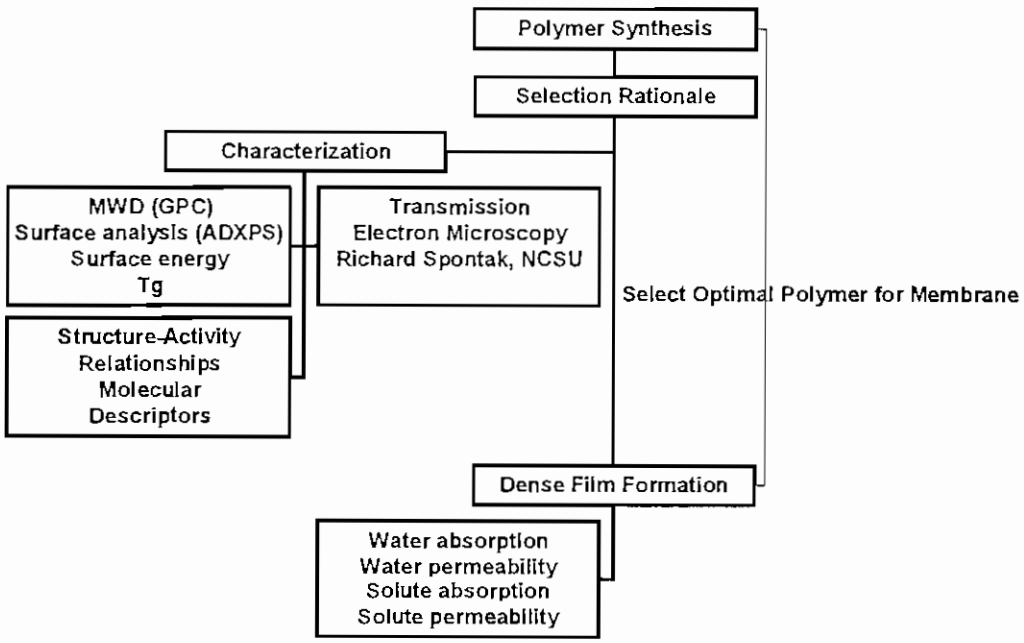

Figure 4. Overview of Research Tasks Related to Block Copolymer Synthesis and Dense Film Testing (MWD = molecular weight distribution; GPC = gel permeation chromatography; ADXPS = Angle-dependent X-ray photoelectron spectroscopy; T_g = glass transition temperature as measured by differential scanning calorimetry (DSC)

The research tasks related to testing of thin-film, composite membranes are shown in Figure 5.

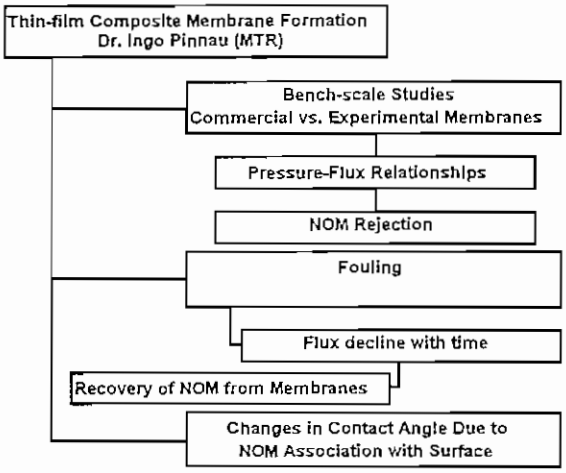

Figure 5. Overview of Research Tasks Related to Thin-film Composite Membrane Testing (MTR= Membrane Technology & Research, Inc.)

Initial Results with PFOA Thin-film Composite Membrane

At the start of this research, a sample of PFOA was sent to Dr. Pinnau of Membrane Research and Technology. It was solvent (Freon-113) cast onto a polysulfone support to provide an initial test of the fouling resistance of a thin-film composite membrane (TFCM) based on low surface tension properties. A 10.2 × 15.2 cm sheet of this experimental membrane was placed in an Osmonics test cell. The test cell was connected to a feed reservoir that contained a 4-L solution of NOM in organic-free, deionized water (OFDW). Both the permeate and concentrate were returned in order to operate the cell in a batch, recycle mode. More details of the experimental set-up will be provided in a later section dealing with follow-up tests of other experimental TFCMs.

The source of NOM was the Suwanee River in Georgia. It was concentrated through reverse osmosis (recycle of concentrate and discard of permeate) and freeze dried until use[9]. The sample was then reconstituted in OFDW to provide a total organic carbon (TOC) concentration (measured with a Shimadzu TOC 5000) of 4.7 mg/L in the feed reservoir.

The Osmonics test cell was pressurized to 8.5 atm (125 psi). Not surprisingly, the hydrophobic nature of the PFOA thin film prevented water permeation through the membrane. In effect, this first TFCM experiment provided confirmation of the expected behavior without addition of a hydrophilic polymer in the proposed block copolymer formulation.

Two other observations from this initial experiment are important to the remainder of the research work. First, the TOC in the feed reservoir decreased from 4.7 to 3.6 mg/L over 50 hours of circulation. Thus, the hydrophobic surface did not prevent NOM accumulation. This should not be surprising given that about 70% of the Suwanee River NOM is hydrophobic based on the operational definition of capture on XAD-8 resin[10]. However, no experiments were conducted to determine the efficacy of removing the accumulated NOM: the low surface tension of PFOA should minimize adhesive forces and thus NOM should not be held strongly.

The second important observation was in regard to the morphology of the skin layer. A scanning electron micrograph (SEM) of the surface revealed a wavy texture, possibly because the low surface tension produced beading of PFOA on the support layer. Undoubtedly, the surface was uneven and this could have accounted for some of the NOM accumulation. Moreover, the PFOA layer was pushed into the microporous support structure after pressurization. The T_g of PFOA was found to be about -15 °C which means that PFOA has a rubbery texture at room temperature and thus can easily be compacted under pressure. These findings led to choosing an alternative low surface energy, fluorocarbon polymer block with a T_g >> room temperature and thus would form a more rigid, less easily deformed membrane material. It was decided, therefore, to polymerize 1,1-dihydroperfluorooctyl methacrylate (FOMA). PFOMA has a T_g of about 50 °C but has a surface energy comparable to PFOA[11].

Block Copolymer Synthesis and Characterization

Polymerization Techniques

Two free radical polymerization techniques — iniferter and atom transfer radical polymerization (ATRP) — were used[12]. These offer the ability to control the polymer

structure and functionality, thus affording polymers with narrow polydispersities, targeted molecular weights and complex architectures.

The term "iniferter" derives from the three functions of the compound: *ini*tiator, chain trans*fer* agent, and reversible *ter*minating agent of the polymer chain. The last of these functions allows for the synthesis of block copolymers. A photoactive compound is used that upon photolysis yields the initiating fragment (R•) and a stable free radical species (S•), typically a thiuram, which serves as the reversible capping agent. Iniferter polymerizations typically give molecular weight polydispersity indices (PDIs) of 1.4 – 1.8. The iniferter technique is effective for the synthesis of a wide range of hydrophilic, lipophilic and fluorocarbon polymers including poly (2-dimethylaminoethyl methacrylate) (PDMAEMA), poly(2-hydroxyethyl methacrylate (PHEMA), and poly(1,1-dihydroperfluorooctyl methacrylate) (PFOMA), all of which were of interest in formulation of block copolymers in this research.

In contrast to the iniferter technique, ATRP employs a haloalkane that serves to help as the initiator along with a copper (I) catalyst and a dipyridyl ligand that serves to help solubilize the copper catalyst. ATRP polymerizations are typically run at 80 - 130 °C. The initiation step occurs by the abstraction of the halogen atom from the haloalkane by the copper (I) catalyst giving a carbon centered radical and copper (II). PDIs of less than 1.3 are typical. ATRP has proven effective for polymerization of a broad range of lipophilic hydrocarbon monomers including acrylates and methacrylates as well as fluorocarbon monomers such as FOMA and 1,1',2,2'-tetrahydroperfluorooctlyacrylate (TAN)[12], all of which were candidates for block copolymer formulations in this research. However, as was found in the early stages of this research, complexation of the copper catalyst species to the polar groups in hydrophilic monomers is a problem.

Synthesis of Block Copolymers

The hydrophobic block was PFOMA in most of the syntheses (see later discussion of PTAN on p. 19, a closely related hydrophobic block). The three hydrophilic blocks were poly (acrylic acid) (PAA), poly(2-hydroxyethyl methacrylate (PHEMA) and poly (2-dimethylaminoethyl methacrylate) (PDMAEMA). Their structures are given in Figure 6 and the results of block copolymer syntheses are summarized in Figure 7.

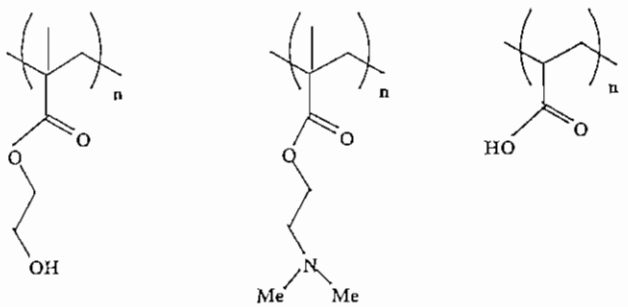

PHEMA PDMAEMA PAA

PHEMA: Poly-hydroxy-ethyl-methacrylate

PDMAEMA: Poly-dimethyl-amino-ethyl-methacrylate

PAA: Poly-acrylic-acid

Figure 6. Hydrophilic polymer structures

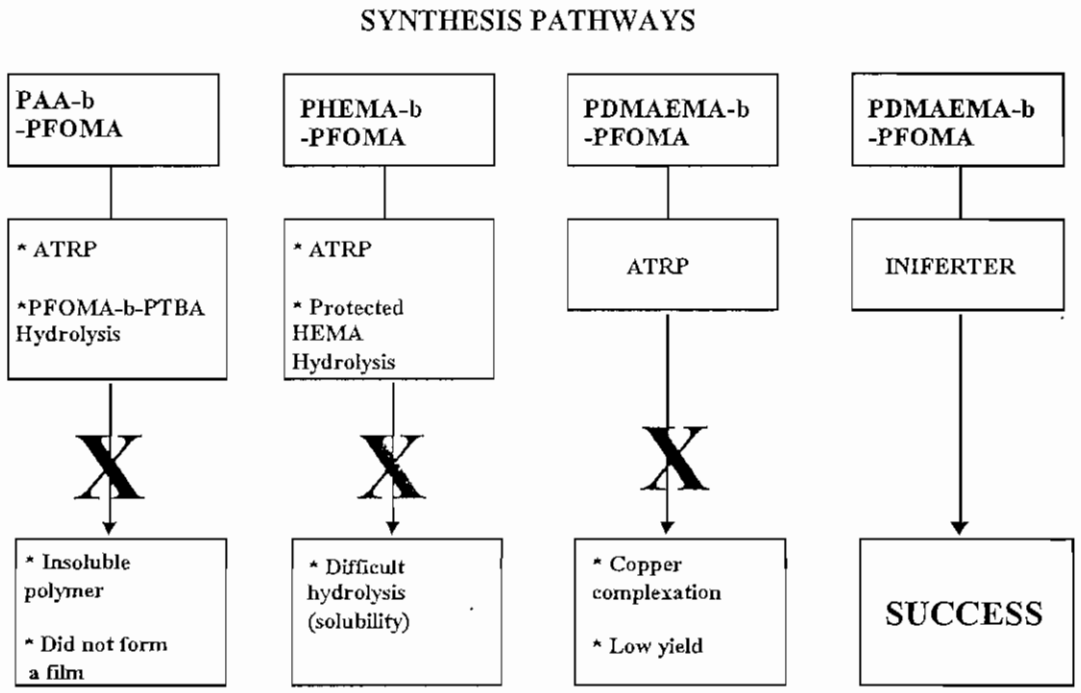

Figure 7. Results of Block Copolymer Syntheses

The analytical techniques used to characterize the block copolymers are listed in Table 1. The results from each technique will only be presented as needed to explain the factors that shaped selection of final choice of block copolymer for further dense film and thin-film testing.

Table 1. Techniques for Physical and Chemical Characterization of Polymers

Analytical Technique	Polymer Characteristic
^{1}H-NMR (nuclear magnetic resonance)	weight fraction of each block; rate of polymerization; MW of the PFOMA (indirectly from MW of hydrophilic block and weight composition)
DSC (differential scanning calorimetry)	Glass transition temperature (T_g) of the polymer. If the T_g < ambient temperature, the polymer is "soft" or "rubbery" and if T_g > ambient temperature, the polymer is "hard" or "glassy.". This affects the mechanical stability of the membrane and the size of transport corridors through the polymer. For block copolymers, two T_g values suggests microphase segregation
SEC (size exclusion chromatography)	Molecular weight distribution (MWD) of each polymer. A low polydispersity index (narrow MWD) is desired. High molecular weight gives mechanical strength.
ADXPS (angle dependent X-ray photoelectron spectroscopy)	Surface segregation of block copolymers, e.g., before wetting, the hydrophobic block should be found near the air/solid interface and the hydrophilic block below but reorganization occurs after wetting favoring migration of the hydrophilic block to the surface.
TEM (transmission electron microscopy)	Morphology resolved at the scale of 10 nm. Selective staining of hydrophilic block in block copolymers can show presence of "domains" that act as channels for water transport. Geometry of the domains (spherical, cylindrical or lamellar) determined by percent composition of block copolymer.

The synthesis of PAA-b-PFOMA (see Figure 7) required a two-step ATRP. In the first step, the poly (tertiary butyl acrylate) (PTBA) was polymerized using the heterogeneous catalyst CuBr(I) / bypyridine / methylbromopropionate; bromo-terminated PTBA then initiates the polymerization of FOMA monomer diluted in α,α,α-trifluorotoluene (TFT) at 100 °C. The next step was selective hydrolysis of PTBA in TFT to yield the desired block copolymer (PAA-b-

PFOMA); this was catalyzed by paratoluene-sulfonicacid (PTSA). The selectivity of the hydrolysis step toward PTBA was verified by showing that the hydrolysis of PTBA homopolymer was much faster than PFOMA homopolymer.

Two copolymers of PTBA-b-PFOMA were formed with a weight fraction of PFOMA of 0.4 and PTBA blocks of 20 and 27 K (according to the weight ratio, the corresponding block sizes for PFOMA were 30 and 35 K). Evidence of phase segregation was provided by ADXPS and TEM: ADXPS showed that the surface was dominated by PFOMA which means that PFOMA segregates at the surface and TEM images showed domains of each phase but no ordered morphology. This was very likely because of the presence of homopolymer.

Unfortunately, it was impossible to synthesize a film of PAA-b-PFOMA because a large amount of insoluble product (50% wt) was formed after hydrolysis and the low solubility of the TFT soluble fraction. This insolubility may be due to reticulation by formation of anhydrides bonds or to the polymer composition (the hydrolysis product of PFOMA homopolymer was also insoluble).

PHEMA-b-PFOMA was synthesized by ATRP (see Figure 7) using the heterogeneous catalyst CuBr(I) / bypyridine / methylbromopropionate. However, strong complexation of copper was encountered in the polymerization of the HEMA monomer and this retarded the polymerization of the second polymer (PFOMA) and caused high recovery (50%) of the homopolymer. Two attempts were made to solve this problem by polymerizing a protected HEMA (*i.e.*, tri-methylsiloxy ethyl methacrylate) and then restoring the HEMA polymer by hydrolysis of the very labile and hydrolyzable tri-methylsiloxy (OSiMe3) group (either in MeOH-water-sulfuric acid at 60 °C or in K_2CO_3 - MeOH at 0 °C)[12]. Neither of these reactions was successful; the low solubility of the block copolymer in the reaction medium may offer an explanation.

The first attempt to synthesize PDMAEMA-b-PFOMA was by ATRP (see Figure 7) using the heterogeneous catalyst CuBr(I) / bypyridine / methylbromopropionate. As was observed in polymerization of HEMA, the DMAEMA monomer complexed strongly with copper. The PDMAEMA homopolymer was well characterized by ^{1}H-NMR. However, it was impossible to measure the molecular weight distribution by GPC in organic solvents because the polymer side chain acted as a strong ligand for the copper

and the solubility of the copper complexed polymer was very low. Polymerization of the second block (PFOMA) was also not satisfactory, probably again owing to the problems of copper complexation. A high fraction of the PDMAEMA homopolymer was recovered showing either a low reaction yield when forming bromo terminated PDMAEMA in the first step or a low initiating efficiency of the first block during the second step (PFOMA block synthesis). Although the diblock (PDMAEMA-b-PFOMA) was isolated and characterized by ^{1}H-NMR, the composition was different than had been expected from ATRP.

The second attempt to polymerize PDMAEMA-b-PFOMA by the iniferter technique was successful (see Figure 7). The details of the reaction pathway are given in Figure 8. In this synthetic technique the PDMAEMA block was synthesized first using the photochemical iniferter benzyl N,N-diethyldithiocarbamate (BDC). After the formation of the first block is complete, the polymer is isolated, purified, and characterized. The second block of the diblock copolymer is then synthesized by dissolving the first block, adding the second monomer (FOMA), and photolyzing. The block copolymer was purified by precipitation in hexane, and soxhlet extraction in methanol to remove any PDMAEMA homopolymer. The composition of each fraction was then measured by ^{1}H-NMR. No block copolymer was extracted: the absence of copolymer fractionation indicated a homogeneous polymer composition in contrast to ATRP results wherein a complex polymer fractionation was observed after purification.

After polymerization of the second block (FOMA monomer), only 60 to 80 wt% of PDMAEMA was integrated into a block copolymer (i.e., 20 to 40% of PDMAEMA was recovered as homopolymer). The presence of PDMAEMA homopolymer suggests that a fraction of PDMAEMA cannot initiate FOMA polymerization.

Supercritical fluid (SCF) extraction in CO_2 was conducted in an attempt to remove some potential PFOMA homopolymer from the block copolymer. This approach was unsuccessful because block copolymer was soluble in CO_2 under the conditions of extraction.

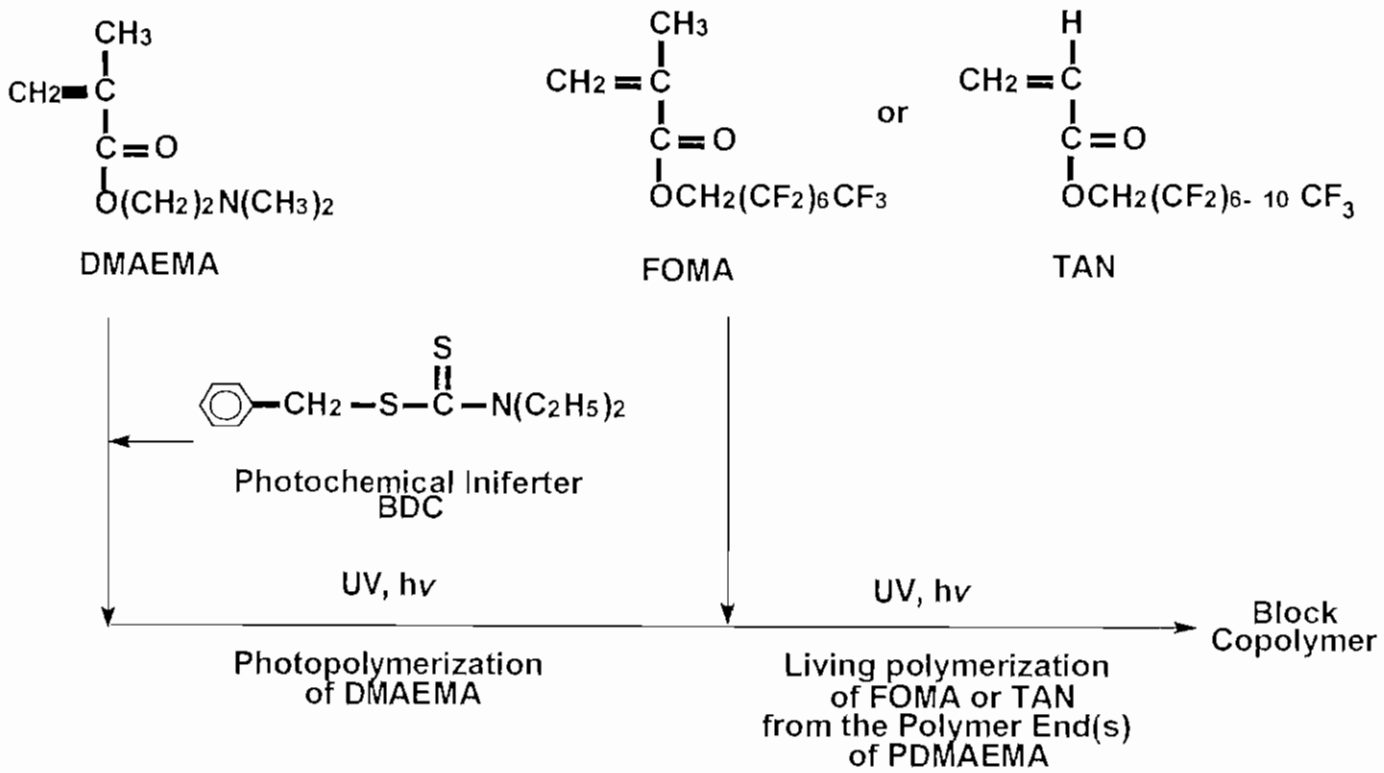

Figure 8. Iniferter synthesis pathway for PDMAEMA-b-PFOMA diblock copolymers

PDMAEMA-b-FOMA was also soluble in TFT and Freon-113 and insoluble in the usual organic solvents tested. It forms clear thin films which can be solvent cast in Freon-113 or TFT. The best support found to minimize the film adhesion on the casting plate was poly-fluoro-ethylene-propylene (other supports tested were glass, aluminum and PTFE). The films appeared to be quite resistant in the dry state and when swollen by water, highly flexible (not brittle).

The weight percent of PDMAEMA and the estimated molecular weight (MW) of the two blocks in the first five PDMAEMA-b-PFOMA samples that were synthesized are listed in Table 2.

Table 2. Estimated weight fraction of PDMAEMA in PDMAEMA-b-PFOMA samples and corresponding MWs of each block

Sample No.	$f_{w,D}$: PDMAEMA weight fraction	PDMAEMA MW (1) Kg/mol	PFOMA MW (2) Kg/mol
#1	0.26	29	82
#2	0.42	29	40
#3	0.38	27	51
#4	0.40	32	47
#5	0.29	27	67

PDMAEMA-b-PFOMA Composition: (1) Calculated MW = [M] / [I] . Conv., (2) MW = $(1-f_{w,D})/ f_{w,D} . MW_{PDMAEMA}$

As will be shown in more detail later, water uptake by the polymer is a good indicator of water permeation rate in membrane applications. Water sorption experiments were conducted with the PFOMA homopolymer and three PDMAEMA-b-PFOMA copolymers containing 5% , 26%, and 42% by weight of the PDMAEMA. The water uptake results are presented in Table 3. As expected, water uptake was negligible for PFOMA and it increased as the percent by weight of hydrophilic block increased. These data suggest that the 26 and 42% PDMAEMA block copolymers would permeate water.

Table 3. Percent water uptake (percent increase in weight of polymer sample) for PFOMA homopolymer and three different PDMAEMA-b-PFOMA compositions

Percent by weight PDMAEMA	% Water Uptake
0	1.3
5	6
26	25
42	100

The results of ADXPS measurements for the 26% and 42% wt PDMAEMA are given in Figures 9 and 10, respectively. They show that the surface was composed of only PFOMA polymer. This can be explained by a strong phase segregation of FOMA at the surface. Phase segregation was also confirmed by DSC on Sample 2 (see Table 2 for sample decription); that is, two values of Tg (21 °C for PDMAEMA and 40 °C for PFOMA) were found.

Thermogravimetric analysis (TGA) showed that the polymer started to decompose above 270 °C in air or nitrogen. Therefore, films can be annealed well above the T_g without any risk of degradation.

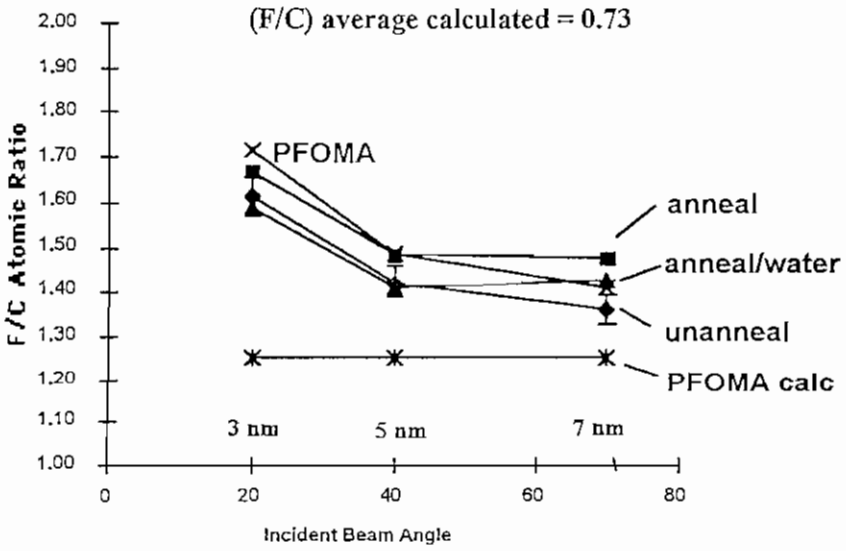

Figure 9. ADXPS Results for PDMAEMA-b-PFOMA, 26% wt PDMAEMA

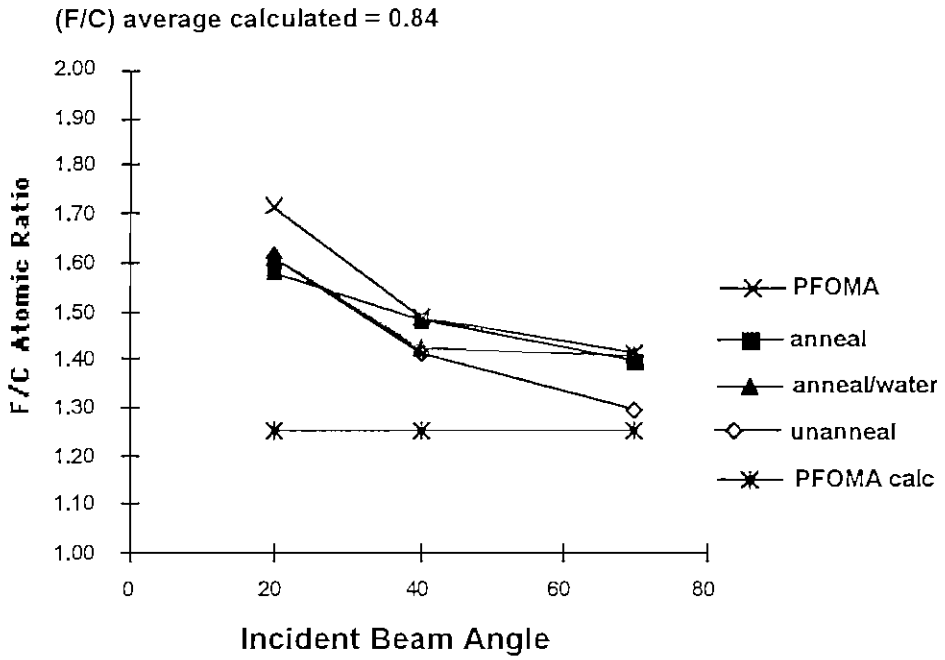

Figure 10. ADXPS Results for PDMAEMA-b-PFOMA, 42% wt PDMAEMA

The kinetics of polymerization were measured in order to know when to stop the polymerization to control the molecular weight of each block. For polymerization of DMAEMA, the rate of propagation was constant, i.e., the radical concentration was constant. This would suggest that no side termination reaction occurred because radical concentration would have otherwise decreased quickly, as would the rate of propagation. However, in the case of FOMA polymerization, the conversion curve leveled out around 20% conversion.

Figure 8 also indicates that the same iniferter technique was used to synthesize PDMAEMA-PTAN [poly(1,1,2,2-tetrahydroperfluorooctyl acrylate)] triblock copolymers (PTAN-b-PDMAEMA-b-PTAN). Polymers prepared from PFOMA (a methacrylate) have no long range order in the fluorinated phase while those prepared from PTAN (an acrylate) have crystalline regions in the fluorocarbon phase. Even though the two polymers have highly similar chemical structure, the PTAN materials have less side chain branching (i.e., defects) than PFOMA, and the PTAN side chains can crystallize. The

crystallites may act to improve the registry of the fluorocarbon molecules with each other, thereby improving the registry (i.e., definition) of the hydrophilic regions since the fluorocarbon and hydrophilic parts of the molecules are connected to each other. We also have data on a triblock represented by PFOMA-b-PDMAEMA-b-PFOMA. Diblock materials can apparently micellize at relatively low hydrophilic contents and perhaps migrate away from the surface of the membranes. However, the triblock materials appear to exhibit a lesser tendency to do this and permit, therefore, the incorporation of higher levels of hydrophilic content in the block copolymer which should lead to higher water flux.

Morphological Analysis: Transmission Electron Microscopy (TEM) Results

A transmission electron micrographs (TEM) of the first film made of PDMAEMA (29 Kg/mol)-b-PFOMA(82 Kg/mol) containing 26 wt% of DMAEMA is represented in Figure 11. It shows a cylindrical structure. The bands represent the cylinders cut along their axis of symmetry and the dots represent the cross section of the cylinders. The white domains are formed of the PFOMA matrix while the black domains are the cylinders formed of PDMAEA. The diameter of these cylinders can be estimated using the equation from Meier[13]:

$$R = \alpha K(MW)^{0.5} \qquad (1)$$

where

R = the radius of the sphere or cylinder

α = factor to account for chains strained at the interface (values range from 1 to 1.5)

$K = r_o/(MW)^{0.5}$ is an experimental constant relating the unperturbed root mean square end-to-end distance (r_o) to the molecular weight, MW.

K will increase if the polymer is charged because charged chain segments repulse each other. Typical values of K for polymethacrylates can be found in the literature[14] and vary depending of the alkyl substituent from 0.05 (i.e. for polyoctylmethacrylate) to 0.09 (i.e., for polymethacrylicacid). It was not possible to find the K value of PDMAEMA in the literature. The characteristic dimension was estimated using the extremes of K as given by

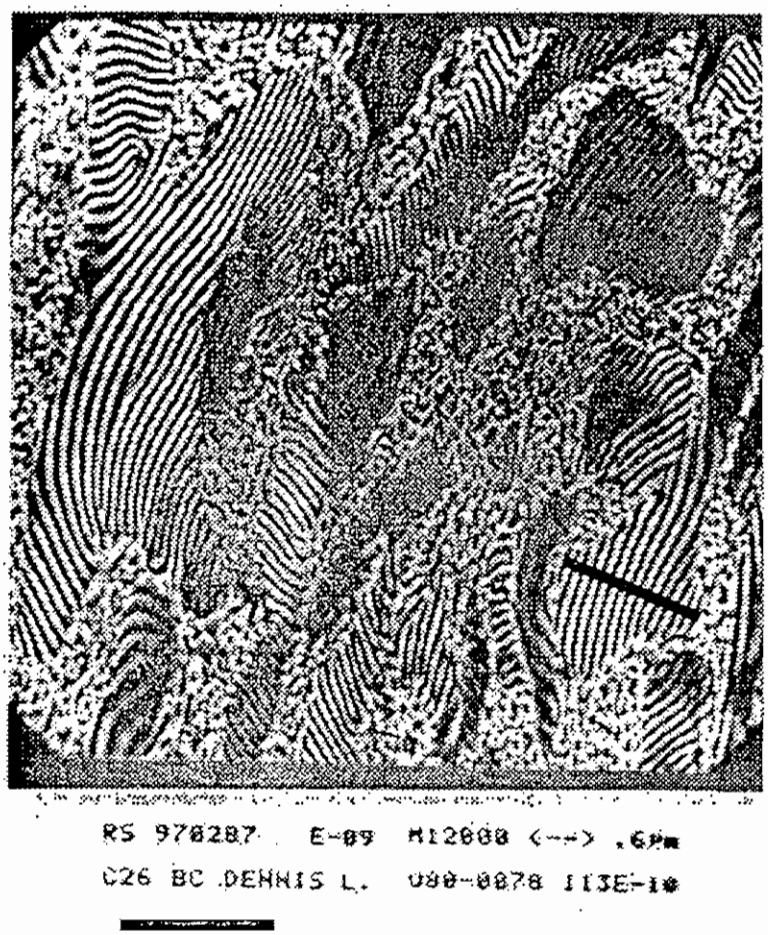

Figure 11. TEM picture of a film made of PDMAEMA(29 Kg/mol)-b-PFOMA (82 Kg/mol) containing 26 wt% of PDMAEMA

the values above and an average α value of 1.25. The diameter calculated from Equation 1 was then compared to the size of the cylinders measured by image analysis of the TEM picture. The results are presented in Table 4.

Table 4. Estimates of Hydrophilic Channel Diameter

α	MW PFOMA (g/mol)	K_{min}	K_{max}	R (nm)	Channel Diameter (nm)	
					Eq. 1	TEM Image Analysis
1.25	29000	0.05	na	11	22	40 to 50
1.25	29000	na	0.09	20	40	40 to 50

The agreement between the experimental and calculated values is acceptable, especially for high values of K. It is to be noted that the amino group of PDMAEMA can be easily protonated in acid conditions and that, in such a case a large K value would be expected.

TEMs were obtained for unexposed (*i.e.*, as cast) and water-exposed samples of four copolymer compositions: PDMAEMA(29% wt, 55 mol%)-b-PFOMA, PDMAEMA(40% wt, 67 mol%)-b-PFOMA, PFOMA-b-PDMAEMA(59 mol%)-b-PFOMA, and PTAN-b-PDMAEMA(38% wt, 69 mol%)-b-PTAN. Each of these four samples was cast from 10-20 (w/v) % solution of Freon-113 with slow evaporation of solvent. To determine whether any morphological rearrangement occurs in the presence of water, half of each film sample was exposed to water while the other half was left unexposed to water. The following procedure was used for the samples that were exposed to water: the samples were first soaked in ultrapure water for 6 hours and then dried in a vacuum oven at ambient temperature for 1 hour to avoid problems with the cryoultramicrotome. All samples were cryoultramicrotomed and imaged by TEM with the assistance of Dr. Richard Spontak of NCSU.

The representative images displayed in Figures 12-15 show that all samples are microphase-separated. The hydrophilic PDMAEMA block is the dark phase, and the fluorinated block (PFOMA or PTAN) is the light phase. Both PDMAEMA-b-PFOMA diblock copolymers, shown in Figures 12 and 13, exhibit non-classical, nondispersed morphologies. The hydrophilic domains are present as dark cylindrical-shaped channels in the unexposed and water-exposed PDMAEMA(55 mol%)-b-PFOMA samples shown in Figures 12a and b, respectively. There are no obvious differences in morphology between the unexposed and water-exposed samples. The unexposed and water-exposed PDMAEMA(67 mol%)-b-PFOMA samples, shown in Figures 13a and 13b, respectively, appear to have a somewhat three-dimensional morphological structure. The presence of dark cylindrical-like channels can still be observed in these images and the morphologies for unexposed and water-exposed samples appear similar to each other.

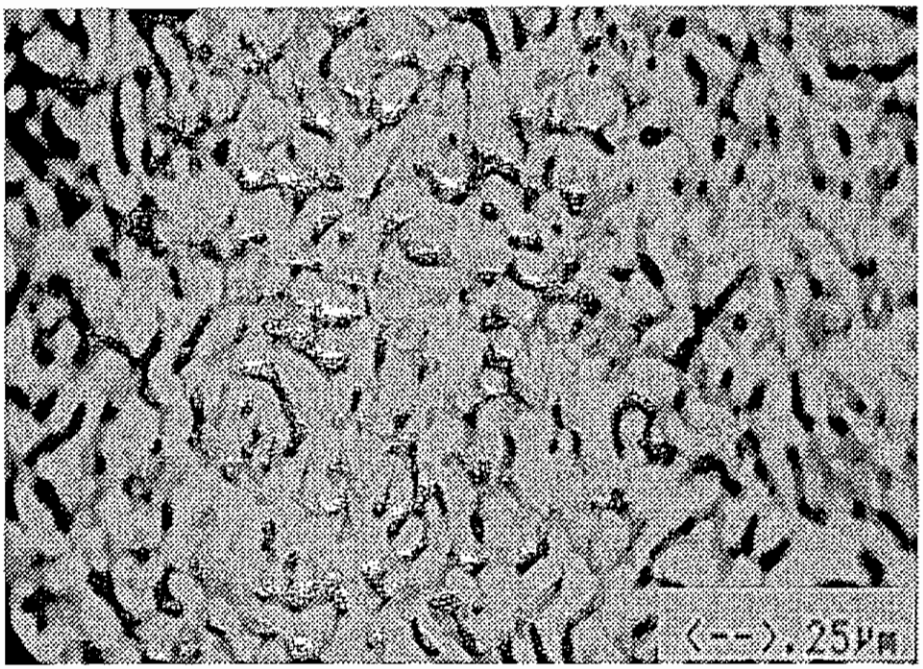

Figure 12a. PDMAEMA(55 mol%)-b-PFOMA morphology: unexposed to water

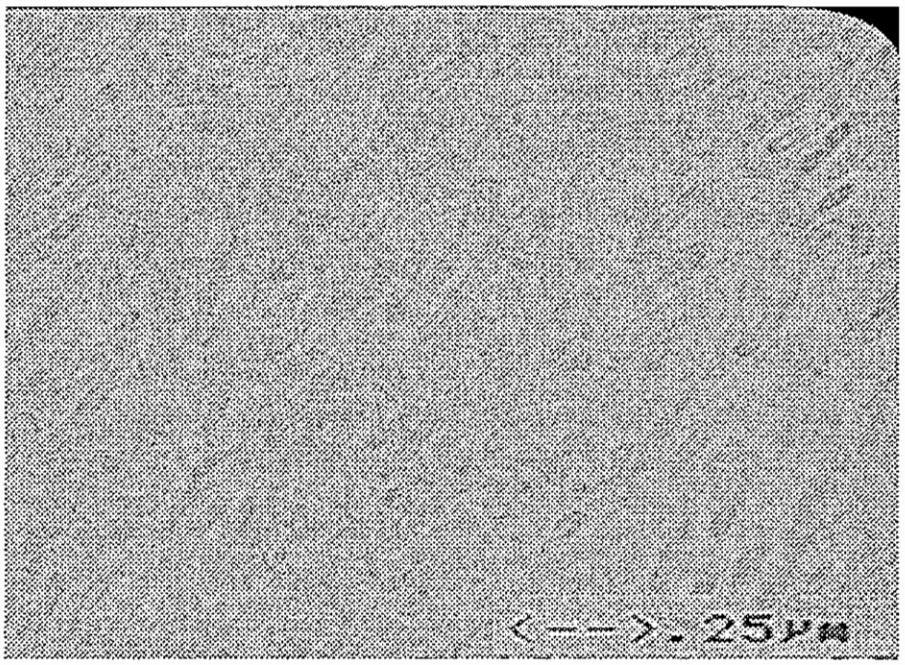

Figure 12b. PDMAEMA(55 mol%)-b-PFOMA morphology: exposed to water

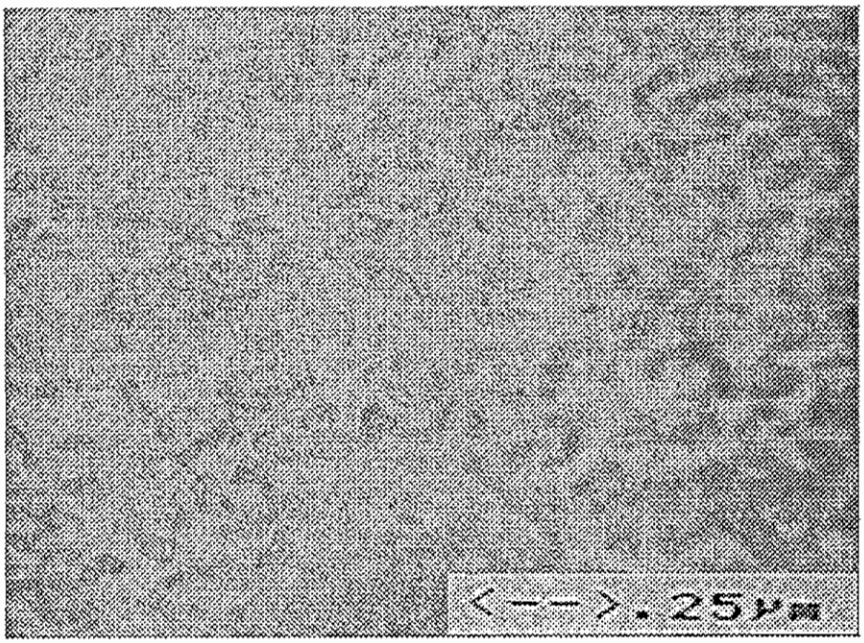

Figure 13a. PDMAEMA(67 mol%)-b-PFOMA morphology: unexposed to water

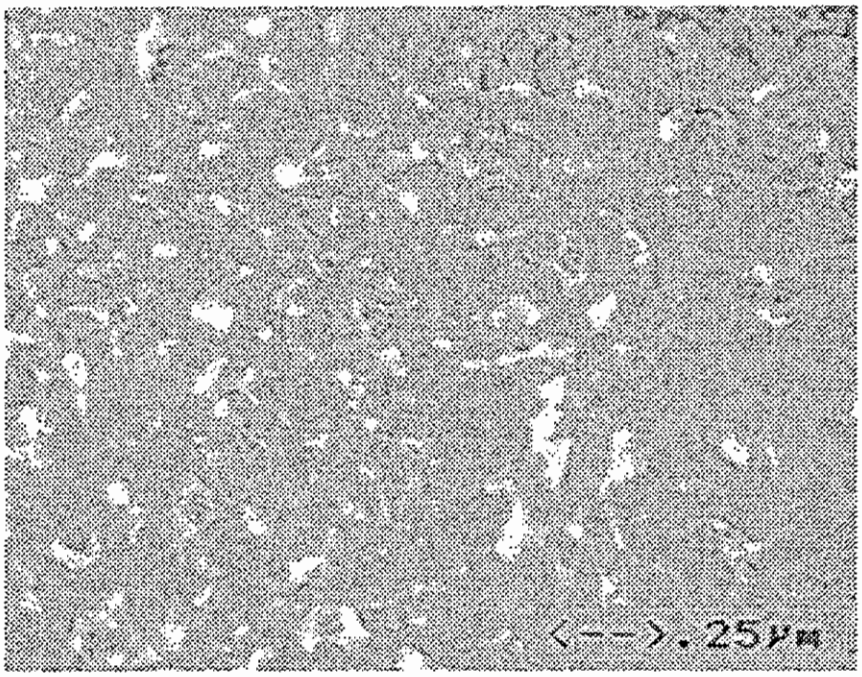

Figure 13b: PDMAEMA(67 mol%)-b-PFOMA morphology: exposed to water

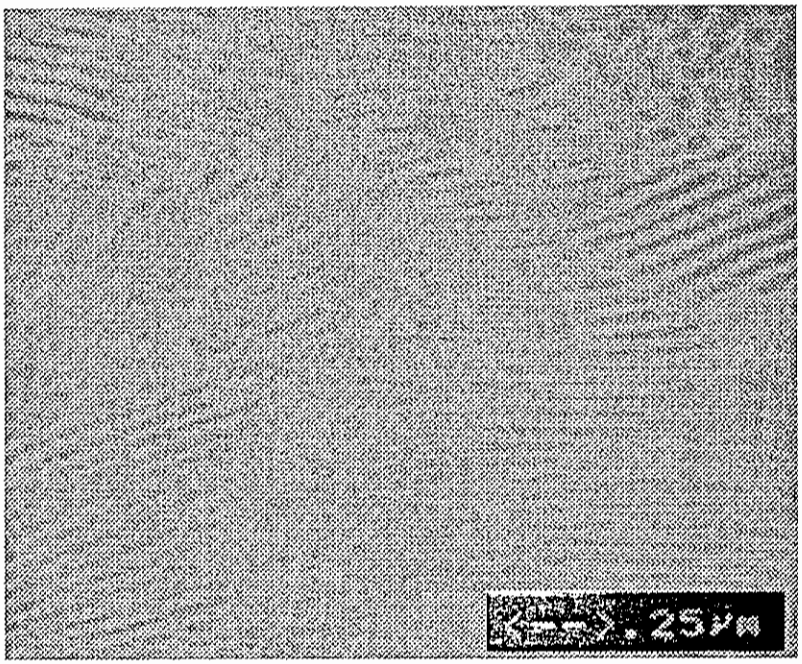

Figure 14a. PFOMA-b-PDMAEMA(59 mol%)-b-PFOMA: unexposed to water

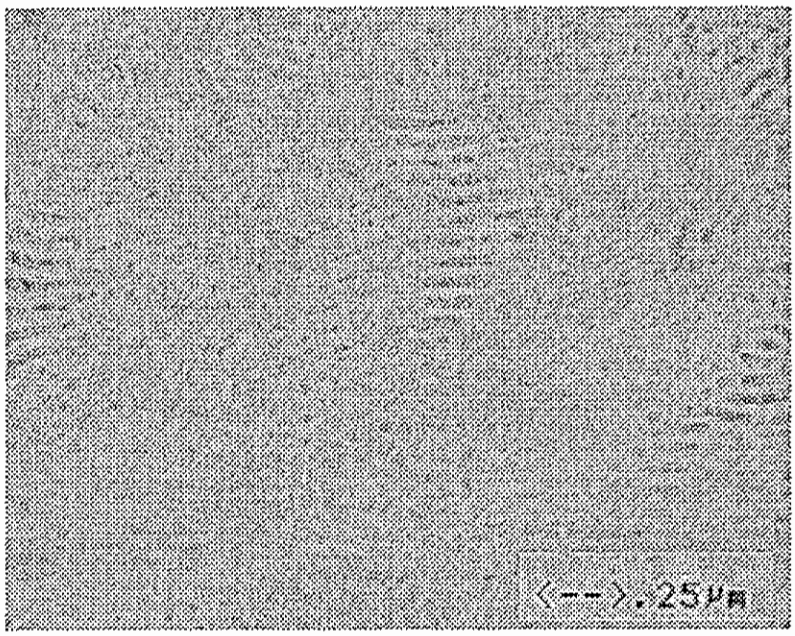

Figure 14b. PFOMA-b-PDMAEMA(59 mol%)-b-PFOMA morphology: exposed to water

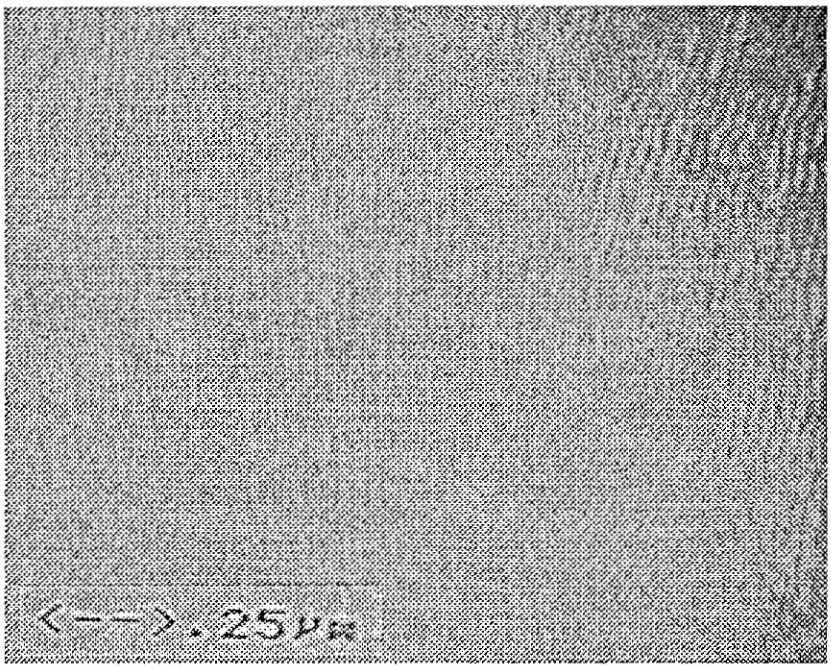

Figure 15a. PTAN-b-PDMAEMA(69 mol%)-b-PTAN: unexposed to water

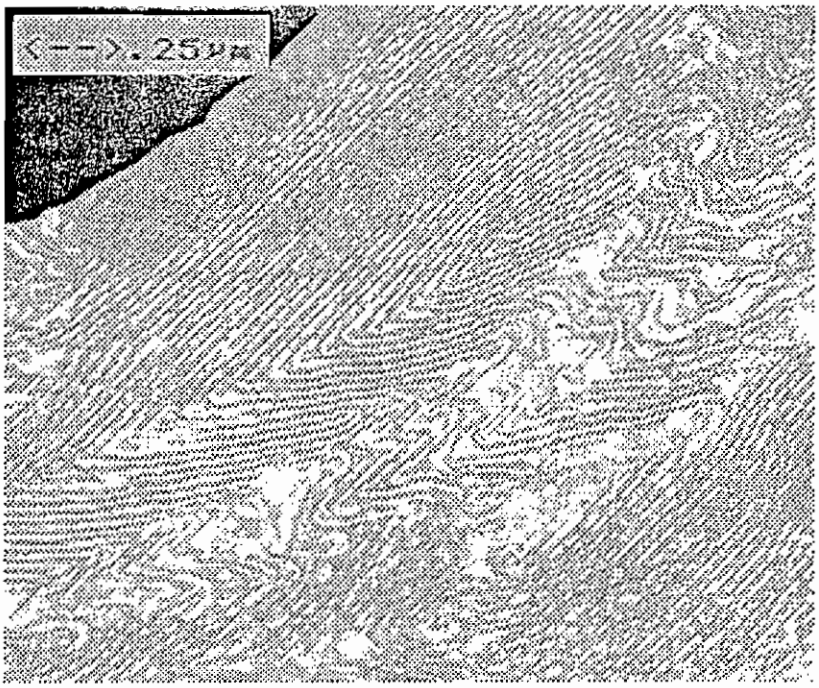

Figure 15b. PTAN-b-PDMAEMA(69 mol%)-b-PTAN morphology: exposed to water

The PDMAEMA-b-PFOMA-b-PFOMA triblock copolymer exhibits a cylindrical morphology for both unexposed and water-exposed samples. (Figure 14). Regions of cylinders which are both parallel to and normal to the plane of the paper can be observed in Figures 14 a and b, implying that these samples have no long-range order. In contrast to the PFOMA-based materials, the PTAN-b-PDMAEMA-b-PTAN triblock copolymer exhibits a classical lamellar morphology in both the unexposed and water-exposed states shown in Figures 15a and b, respectively. Neither triblock showed significant morphological rearrangement upon exposure to water.

Negatives were digitized and channel sizes were measured using Digitalmicrograph (Gatan, Inc. Pleasanton, CA). The hydrophilic PDMAEMA channel sizes ranged from approximately 15 to 30 nm for all of the copolymers, with the narrowest channel sizes being observed for the PTAN-b-PDMAEMA-b-PTAN triblock copolymer.

Dense Film Characteristics

The general procedure for preparation of dense films was:

1. Dissolve the block copolymers with the PFOMA hydrophobic block in 5-10 w/v % of Freon 113 and those with PTAN hydrophobic block in 5-10 w/v % of TFT, both at room temperature
2. Filter the casting solution through a 1 μm glass fiber filter
3. Attach a glass ring (10-14 cm in diameter and 2-3 cm in height) to a flat Teflon sheet (casting plate) with modeling clay.
4. Pour the filtered casting solution into the casting ring
5. Cover the casting ring with a glass plate to control the rate of solvent evaporation
6. Wait for the film to dry (2-7 days depending of film thickness)
7. Remove the glass ring from the Teflon casting plate and soak the casting plate in ultrapure water to soften the film
8. Remove the film from the casting plate and sandwich it between filter paper for drying Film thickness and film diameter ranged from 44-180 μm and from 10-14 cm, respectively.

The following tests were made: (1) equilibrium water uptake (film suspended in water); (2) pure water permeation in dead-end filtration cell; (3) NaCl diffusion (desorption of NaCl from suspended film into water); and partitioning of NaCl and NOM (sorption from water into film).

Water Uptake

The results in Figures 16 and 17 show that water uptake and pressure normalized flux both increased as the PDMAEMA content (i.e., hydrophilic structure content) increased. Since PFOMA had less than 2 wt% water uptake and immeasurably low water flux, water can be assumed to sorb into and permeate through the hydrophilic PDMAEMA domains. Figure 18 shows a plot of pressure-normalized flux versus water uptake for this family of PDMAEMA copolymers. Water flux clearly increases with increasing water uptake. Hence, water sorption experiments have proven to be a useful screening test for predicting which materials will have adequate water flux for further characterization.

These block copolymer films are non-porous, but the water fluxes produced were in the same range as those for commercial porous membranes such as Hydranautics NTR-7450 and Millipore 1000 NMWL regenerated cellulose [both pressure- normalized fluxes are ca. 6 L/(m^2-h-atm)]. Therefore, the pure water fluxes for these materials are sufficient for practical applications.

In summary, the above results indicated that pure water uptake and permeation in these films depends on both the hydrophilic content and microstructure of the block copolymer film. Samples which sorbed greater quantities of water also had higher pure water fluxes.

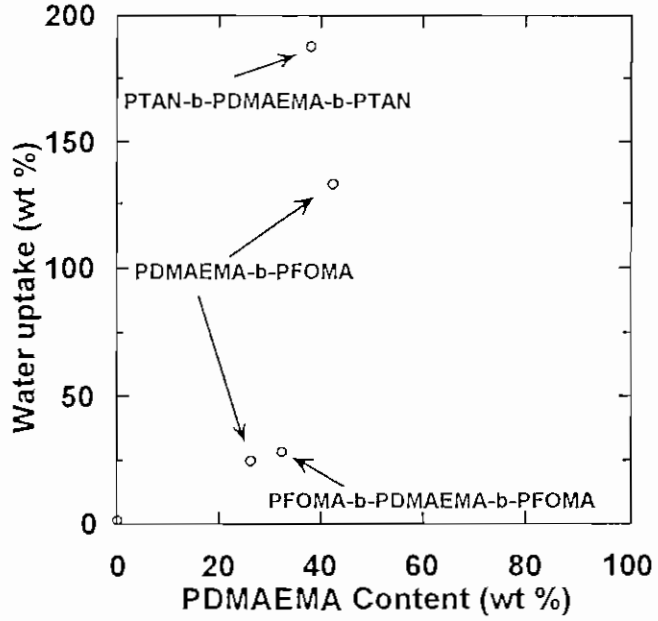

Figure 16. Relationship between water uptake and PDMAEMA content

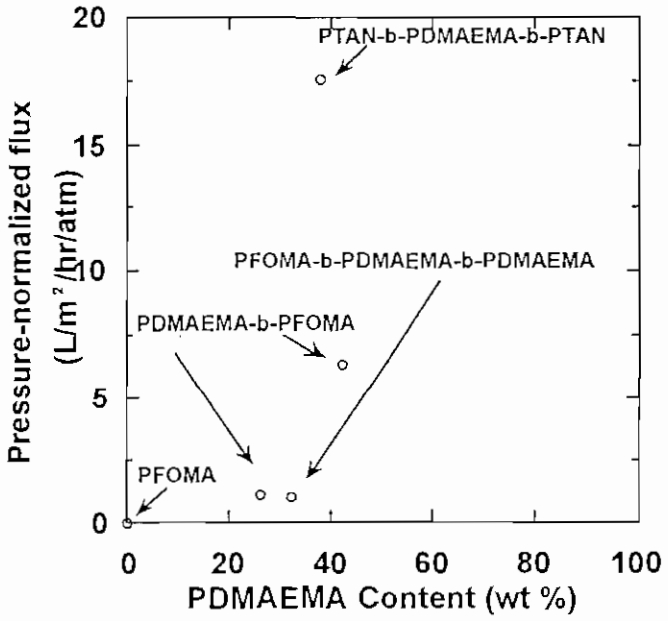

Figure 17. Relationship between pressure-normalized flux and PDMAEMA content

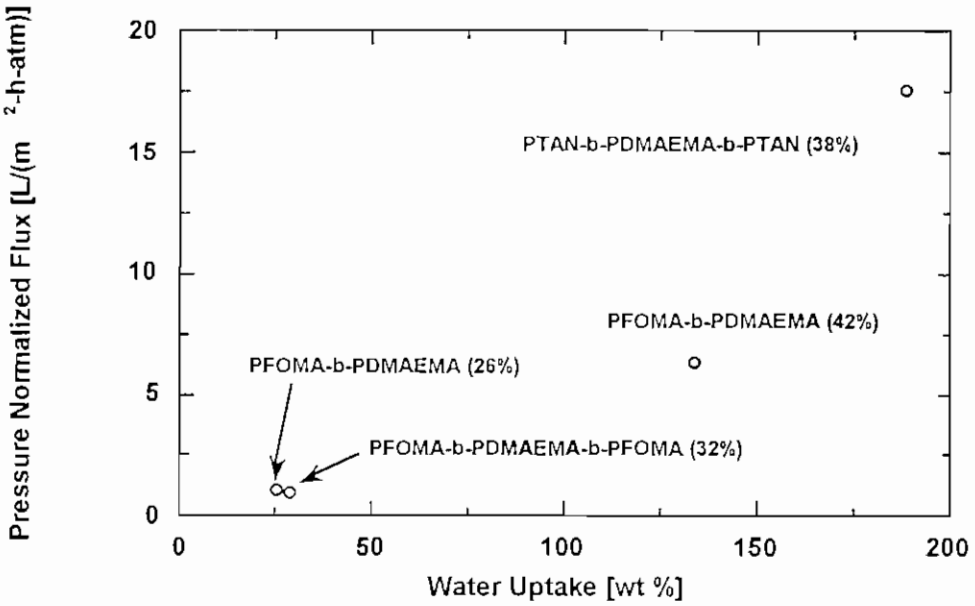

Figure 18: Dependence of pressure-normalized flux upon water uptake.

Sodium Chloride Diffusion and Partitioning

Sodium chloride diffusion and partition coefficients were determined in a sodium chloride desorption experiment. First, the film was equilibrated in a 5 wt% NaCl solution. Then its surface was blotted to remove excess surface salt, and it was immersed in ion-free water from a Millipore system. Conductivity was monitored as a function of time, and the amount of salt released into the water was determined from a salt-conductivity calibration curve. Diffusion coefficients were calculated using classical Fickian analysis[15], and the distribution coefficient was calculated from the equilibrium amount of salt released into the ion-free water.

The salt diffusion coefficients for the PDMAEMA-b-PFOMA diblock copolymers containing 26 and 42 wt% PDMAEMA were 5.5×10^{-7} and 4.1×10^{-8} cm^2/s, respectively. The salt distribution coefficient for the 26 wt% PDMAEMA diblock copolymer was 0.41 [(g NaCl/cm^3 film)/(g NaCl/cm^3 solution)], while the distribution coefficient for the 42% PDMAEMA diblock copolymer was 0.62. Since salt permeability can be estimated as the product of the salt diffusion coefficient, D, and the salt distribution

coefficent, K, the 26 wt% and 42 wt% PDMAEMA diblock copolymers had salt permeabilities of 2.25×10^{-7} and 2.5×10^{-8}, respectively.

Determination of NOM Partitioning Coefficient

The NOM-containing solution used in partitioning experiments was settled-filtered water from the P. O. Hoffer water treatment plant in Fayetteville, NC; the source is the Cape Fear river. NOM was preconcentrated by passing the water through a reverse osmosis unit, discarding the permeate and returning the concentrate to the feed reservoir. In less than 1 hour of circulation, nearly a factor of ten increase in NOM concentration was achieved. The purpose of preconcentration was to increase the accuracy of the measurement in difference between the initial and final NOM concentration remaining in batch solution after contact with the dense film.

A flask containing the NOM solution and dense film (7 cm in diameter) was covered and stirred for 48 hours. After this time, the equilibrium concentration of NOM was measured by both total organic carbon (TOC) and UV absorbance at 254 nm. A control experiment was conducted in the same way but with only the 7 cm -diameter film of FEP so as to determine if NOM would adsorb to this casting support material. Three replicate tests were conducted in addition to the control study of FEP partitioning. The results are given in Table 5.

Table 5. Determination of NOM partition coefficient

	Control FEP film	Dense Film of PDMAEMA-b-PFOMA 25.8 Mole % PDMAEMA		
Film Thickness (cm)	0.0127	0.0026	0.0045	0.0068
C_O (UV_{254}) [1]	0.579	0.579	0.563	0.563
C_E (UV_{254}) [1]	0.575	0.532	0.485	0.420
K_{UV} (UV abs/cm^3 film/UV abs /cm^3 solution)	--	17.7	18.57	26.02
C_O (mg/L TOC)	19.83	22.3	NA	NA
C_E (mg/L TOC)	20.90	20.84	NA	NA
K_{TOC} (mg TOC/cm^3 film/mg TOC/cm^3 solution)		14.0		

[1]Measured with a 5 cm cell path semi-microcell

As seen from the small decrease in UV_{254} absorbance upon equilibration, the partitioning of NOM to the FEP is insignificant. In contrast, the decrease in UV_{254} was very easily measured for the experimental dense film. The K values measured by both UV-254 absorbance and TOC agreed fairly well.

Table 6 provides a comparison of K values for different solutes and different dense or thin films. The experimental block copolymer materials sorbed 100 times less NaCl than cellulose acetate. They also sorbed 30-100 times more NOM than NaCl. There was less sorption of NOM on the experimental material than on cellulose acetate although the difference was not as great as for NaCl. The diffusivity of NOM for these materials was not determined because of difficulties in measurement of low concentrations in solution during NOM desorption rate tests. However, it is likely that the diffusivity of NOM is much smaller than of NaCl owing to the larger molecular weight of NOM. If so, the lower D value may offset the higher K value making NOM permeability similar to that of NaCl.

The estimates of K should be interpreted cautiously. It would be important to measure the change in K with the hydrophilic content of the experimental block

Table 6. Comparison of K values for different solutes and membrane materials

Membrane (M) or Dense Film (DF)	Solute	K (g solute/cm^3 film/g solute/cm^3 solution)	Study
DF of (PDMAEMA-PFOMA or PDMAEMA-PTAN)	NaCl	0.2-0.6	This Study
Cellulose Acetate (M)	NaCl	380±50	Lonsdale, et al.[15]
Cellulose Acetate (DF) 26 wt % PDMAEMA -b-74% PFOMA(DF)	NOM Fayetteville, NC (Cape Fear R.)	≈100 ≈21	This Study
Polysulfone PM 30 (M)	NOM Suwannee R.	114 (HA) 67 (FA)	Jucker and Clark[16]
Acrylic copolymer XM50 (M)	NOM Suwannee R.	65(HA) 44 (FA)	Jucker and Clark[16]
Cellulose Acetate (M)	Dichlorobenzene	25	Lonsdale, et al.[15]

copolymers to determine if partitioning is specific to regions occupied by one of the two polymers. The K value from the Jucker and Clark[16] study was calculated by us assuming that the total volume of ultrafiltration membrane was available for partitioning. A later paper by Clark and Lucas[17] used a different approach in which only a small fraction of the volume was assumed available; this results in many orders of magnitude increase in K.

Summary of Dense Film Test Results

The results in Figure 18 indicate as expected that higher water uptake is required to produce high water flux. Higher selectivity is associated with lower salt permeability and requires materials with lower values of K and D. The values of K, D and K × D for the experimental dense film materials are compared those for cellulose acetate dense films in Table 7. While the D values are much higher for the experimental materials, the K values are much lower. The net result is a permeability that is 6 to 60 times lower for the experimental materials than for cellulose acetate. Controlling the block copolymer microstructures to reduce the value of the D may be the best way to design new materials. The microstructure of PFOMA-b- PDMAEMA (42 wt%, 69 mol %) may prove to be a successful example of this design concept.

Table 7. Comparison of D, K and permeability of NaCl for cellulose acetate and the experimental dense film materials

Dense Film Material	$D \times 10^9$ (cm^2/s)	K (g NaCl/cm^3 film/g NaCl/cm^3 solution)	$K \times D \times 10^7$ (cm^2/s) (g NaCl/cm^3 film/g NaCl/cm^3 solution)	Reference
Cellulose Acetate	3.2±0.6	380±50	12.2	Lonsdale, et al.[15]
PDMAEMA-b-PFOMA and PFOMA-b-PDMAEMA-b-PFOMA	300-550	0.2-0.6	0.2-2	This work
PTAN-b-PDMAEMA-b-PTAN	50	0.65	2	This work

Testing of Thin-film Composite Membranes with PDMAEMA-PFOMA Diblocks

Two PDMAEMA-b-PFOMA diblock copolymers containing 29 and 40 wt% PDMAEMA, respectively, were prepared as thin-film composite membranes by Dr. Ingo Pinnau of Membrane Technology and Research in San Diego, CA. The diblock copolymers were wick-coated from a Freon-113 solution (2 % w/v). The PDMAEMA-b-PFOMA layer thickness was determined by SEM to be between 1 and 2 μm.

Rejection of PEG

The rejection of polyethylene glycol (PEG) was measured to have a point of comparison of molecular weight cut-off (MWCO) with a Hydranautics NTR-7450 nanofiltration membrane (sulfonated polysulfone thin-film composite to provide hydrophilic surface). These results were obtained in a crossflow experiment. The filtration system was designed and built by Separations System Technology and had a 30 L feed tank and three small permeation cells (1 × 3 inch membrane area) in series.

Table 8 shows the percent rejections attained for the Hydranautics NTR-7450, two PDMAEMA-b-PFOMA thin-film composite membranes and the microporous polysulfone support when PEG standards of different number-average molecular weight (M_n) were added to the feed tank. Typically, the molecular-weight cut-off of a membrane is determined by plotting PEG rejection vs. PEG molecular weight; the point on this rejection-molecular weight curve where 90% of the PEG is rejected is defined as the molecular weight cut-off. On the basis of the data given in Table 8, it can be implied that the commercial Hydranautics NTR-7450 membrane has the highest selectivity for PEG and the lowest molecular weight cut-off (less than 600 g/mol), while the microporous polysulfone support has the least selectivity for PEG and the highest molecular weight cut-off (between 1000 and 10000 g/mol). The PDMAEMA-b-PFOMA composite membranes containing 40 and 29 wt% PDMAEMA appear to have molecular weight cut-offs slightly greater than and slightly less than 600 g/mol, respectively.

Table 8. PEG Rejection for Commercial and Experimental Membranes

PEG Standard	Hydranautics NTR-7450	PDMAEMA-b-PFOMA (40 wt% PDMAEMA)	PDMAEMA-b-PFOMA (29 wt% PDMAEMA)	Microporous Polysulfone Support
PEG Mn~10,000	99.8			98.2
PEG Mn~1000	97.9			74.7
PEG Mn~600	97.8	88.6	92.7	

NaCl Rejection

The NaCl rejections are compared in Table 9 for the Hydranautics NTR-7450 control membrane and the two thin-film PDMAEMA-b-PFOMA composite membranes containing 29 and 40 wt% PDMAEMA, and the microporous polysulfone support. These results were obtained in the same crossflow test apparatus as described above.

Table 9. Percent rejection of NaCl

Membrane	% NaCl Rejection
Hydranautics NTR -7450 Nanofilter	73,80
29 wt% PDMAEMA-71 wt%PFOMA	74
40 wt% PDMAEMA-60 wt% PFOMA	66
Polysulfone support	7

The NaCl rejection for the two experimental membranes and the commercial Hydranautics membrane were similar. The microporous polysulfone support was not expected to reject NaCl because its function is to serve as a support for the thin block copolymer separating layer without creating resistance to mass transport. These data show that the goal of synthesizing microphase-separated block copolymers with morphologies that would produce high rejection of solutes was achieved.

Ultrapure Water Flux

A series of experiments were conducted in a cross-flow test cell provided by Osmonics that accommodates larger flat sheets than the Separations System Technology test cell. The Osmonics test cell accommodates a 4 × 6 in (10.2 × 15.2 cm) flat sheet

which corresponds to a surface area of about 138 cm^2. The cross-flow velocity was set at about 0.1 m/s. A schematic of the cell set-up is provided in Figure 19. The sample volume in the feed reservoir was 4 L. A fraction of the concentrate was returned to the feed line to the membrane and the remainder was returned to the feed reservoir; this is referred to as the *batch, internal recycle mode* of operation. Percent recovery of water from the membrane system is simulated by the fraction of concentrate that is returned to the feed line. As this fraction increases, the simulated percent recovery water increases because the concentration of foulants applied to the membrane increases as would be true of membrane elements further downstream in a membrane module. In these studies, the goal was to simulate 80% percent recovery of water as described by DiGiano, Arweiler and Riddick[18]. A cold-water coiling coil was used to remove excessive heat produced by the high pressure, centrifugal pump (Webtrol, EZ series). However, the amount of heat generated by this pump made it necessary to operate at about 30°C instead of the target of 22°C.

Ultrapure water was fed to the Osmonics test cell and permeate flux was measured at several times to assure steady-state had been achieved. The transmembrane pressure was increased stepwise to obtain data the shown in Figure 20. The performance of the two experimental membrane materials was compared to the Hydranautics NTR 7450 nanofilter and to the polysulfone support material.

Flowrate increased linearly with transmembrane pressure for each membrane sample. Dividing flowrate by membrane area gives water flux, after which the slope according to the resistance model for filtration would be $1/\mu R_m$ were μ is viscosity and R_m is the resistance of the membrane. The least resistance is seen for polysulfone. This is reasonable because polysulfone serves as the mechanical support layer and has large pores. The flux is greater and the resistance is lower for the PDMAEMA-b-PFOMA (40 wt% PDMAEMA) than for the PDMAEMA-b-PFOMA (29 wt% PDMAEMA) membrane as would be expected because of its greater hydrophilic content. The flux for the Hydranautics membrane results would need to be adjusted upward by about 20% to compare to the experimental membranes because of the effect of higher viscosity at lower

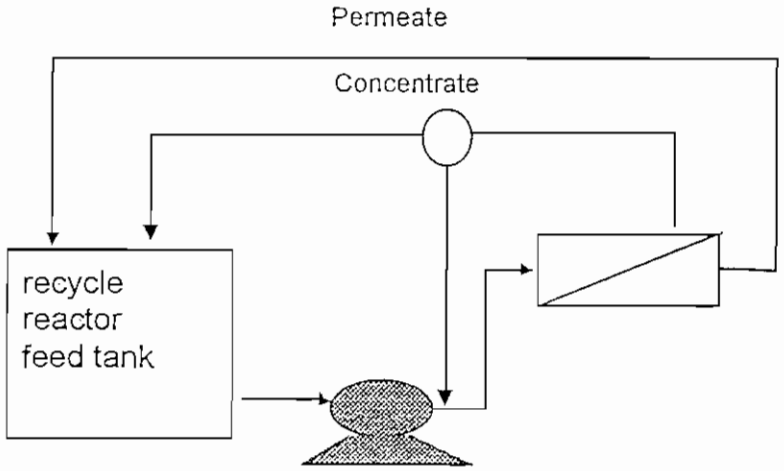

Figure 19. Schematic of batch, internal recycle membrane system

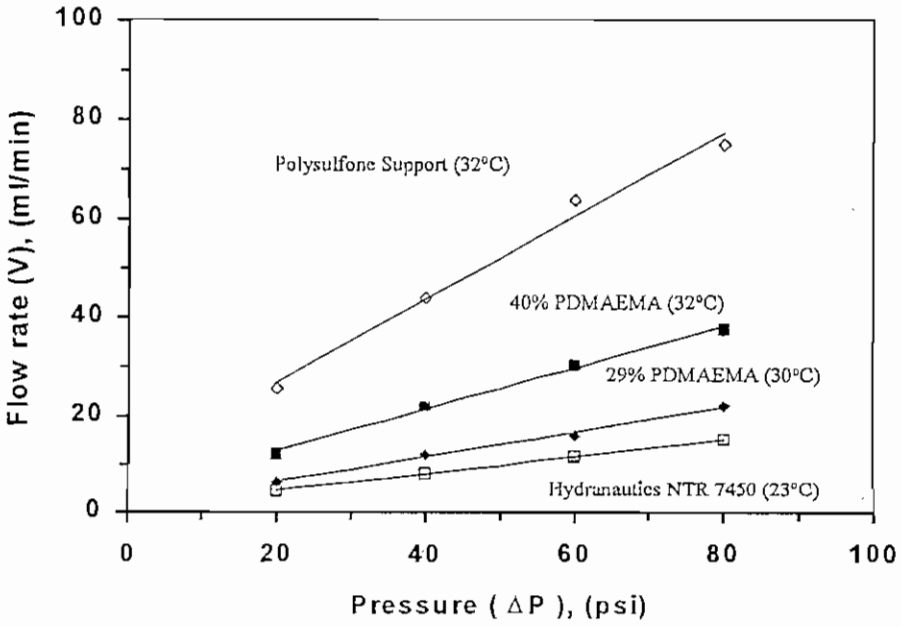

Figure 20. Dependence of membrane permeation rate on transmembrane pressure

temperature of this experiment. Nevertheless, the flux would still be significantly higher for the 40%wt PDMAEMA than for the Hydranautics membrane.

NOM Fouling and Rejection

The same batch, internal recycle mode of membrane operation was used to evaluate NOM fouling and rejection for the two experimental membranes, the Hydranautics NTR 7450, and the polysulfone support material. A batch of settled-filtered water from P. O. Hoffer Water Treatment Plant in Fayetteville, NC (Cape Fear River water) was used to evaluate NOM fouling and rejection. The typical TOC of settled-filtered water was 2.5 mg/L and the UV_{254} absorbance was 0.05 cm^{-1}.

As shown in Figure 21, similar flux decline was observed for all three membrane test systems. Thus the experimental membrane offered no advantage over the Hydranautics membrane. Equally interesting is the observation of flux decline in the polysulfone support material. Cleaning at pH 10.4 with Zenon MC3, an inorganic cleaning solution, did not fully recover flux for any of the three membrane systems. The cleaning cycle consisted of the following steps: (1) circulation of 1 L of cleaning solution through the membrane cell at low pressure for 1 hour; (2) circulation of ultrapure water as a rinse solution for 15 minutes; and repeat of steps (1) and (2).

As also seen from Figure 21, the flux decline after the first cleaning was more severe for the two experimental membranes than for the Hydranautics membrane. Modifications, such as a different choice of hydrophobic polymer or triblock instead of diblock formulation may improve the performance.

Figure 22 indicates that the rejection of NOM as measured by UV-254 nm absorbance was very poor for the experimental membranes compared to the Hydranautics NTR 7450 membrane. This was difficult to explain given that the fouling rates and the NaCl rejection were similar to the Hydranautics membrane. One possibility is imperfections in the thin layer of the block copolymer were responsible; this is likely with the relatively large test sheets required in the Osmonics cell. Another possibility is that the chemical cleaning of this membrane resulted in chemical attack on the block copolymer which compromised the rejection capability. Scanning electron micrographs (SEM) showed raised blotches on the membrane surface after exposure to the MC-3

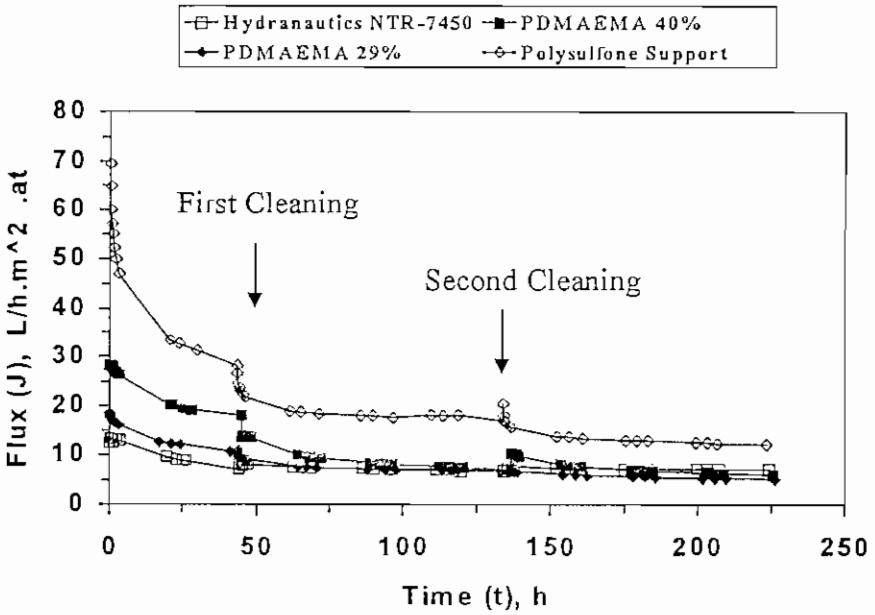

Figure 21. Comparison of flux declines for membranes exposed to NOM-containing water from the P. O. Hoffer Water Treatment Plant in Fayetteville, NC

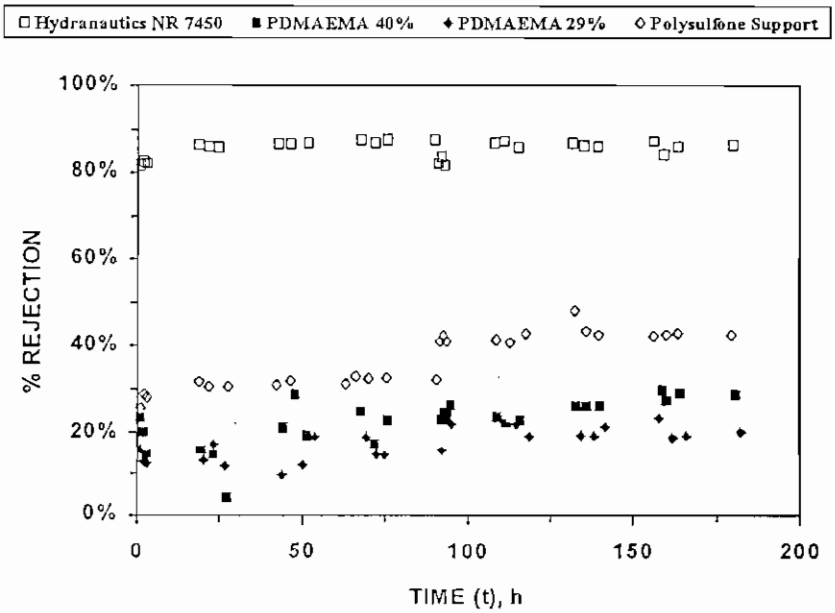

Figure 22. Comparison of NOM rejection as measured by UV_{254} absorbance for membranes exposed to P.O. Hoffer WTP sample

cleaner. It could well be that ester groups within the block copolymers were hydrolyzed at pH 10.5. In addition, there was an increase in solution TOC after exposing the experimental membranes to the cleaning solution at pH 10.5 in static tests that would suggest leaching as well.

The accumulation of NOM on the membrane surface was measured by the decrease in TOC and UV_{254} absorbance in the feed reservoir. This was expressed as a fraction of NOM lost from the feed solution:

$$\text{fraction of NOM lost to membrane} = \frac{(C_o - C_t)V}{C_o V} \qquad (2)$$

where C_o is the TOC concentration or UV_{254} absorbance of the initial feed solution, C_t is the concentration of the corresponding parameter remaining in solution at any time, t, during membrane filtration, and V is the volume of the feed solution. The increase in fraction of NOM lost to the membrane as measured by UV_{254} absorbance during the first run (i.e., before the first cleaning) is given in Figure 23. The same data are provided for the second run (i.e., after the first cleaning) in Figure 24. The rate of NOM accumulation

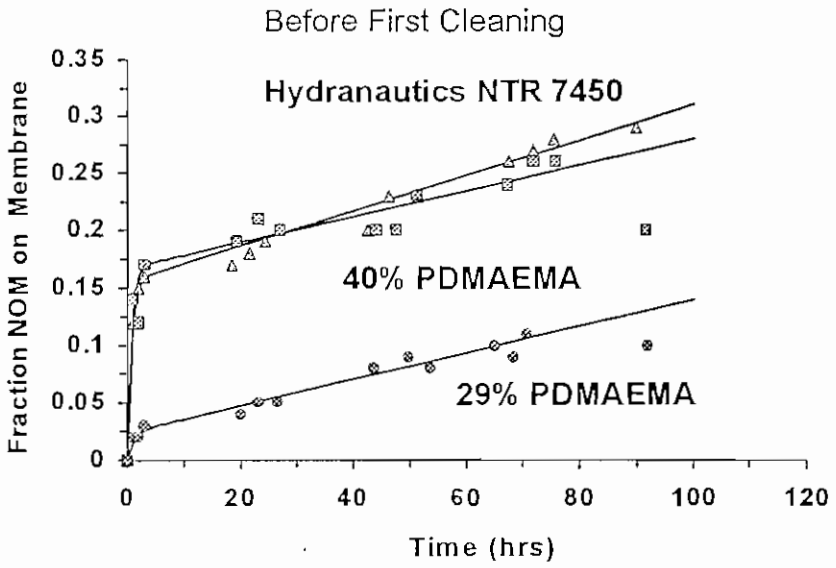

Figure 23. Accumulation of NOM on commercial and experimental membrane surfaces during Run 1

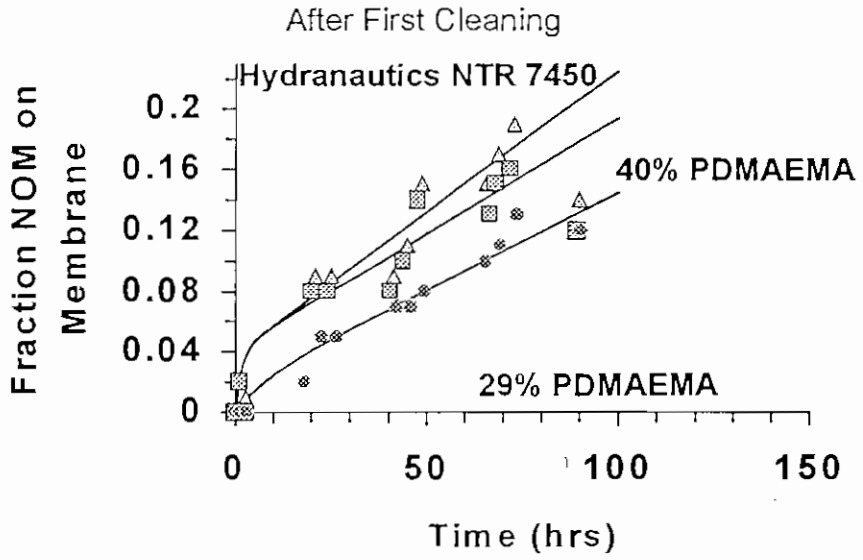

Figure 24. Accumulation of NOM on commercial and experimental membrane surfaces during Run 2

on the experimental membranes generally less than on the commercial membrane but still significant.

The effectiveness of membrane cleaning was measured both by the decrease in NOM (as measured by TOC and UV_{254}) in the batch reservoir and by the mass of NOM recovered in the 1-L volume of recirculated cleaning solution. The percent of NOM in the feed reservoir that fouled the membrane and the efficiency of cleaning are summarized for each membrane in Figure 25. The dark solid bar is the percent of NOM lost from solution to the membrane surface just before the first cleaning (MF1= membrane filtration Run 1). The white solid bar is the percentage of the accumulated NOM that was removed by the cleaning solution. The gray solid bar is the percent of NOM lost from solution to the membrane surface just before the second cleaning (MF2= membrane filtration Run 2). The speckled bar is the percentage of the accumulated NOM during the second run that was removed by the cleaning solution.

Although the extent of fouling is about the same for the experimental membranes and the Hydranautics NTR 7450 membrane, the efficiency of recovery is greater for the

experimental membranes. This may suggest that the block copolymer formulation provided a surface with weaker adhesive forces but more data are needed.

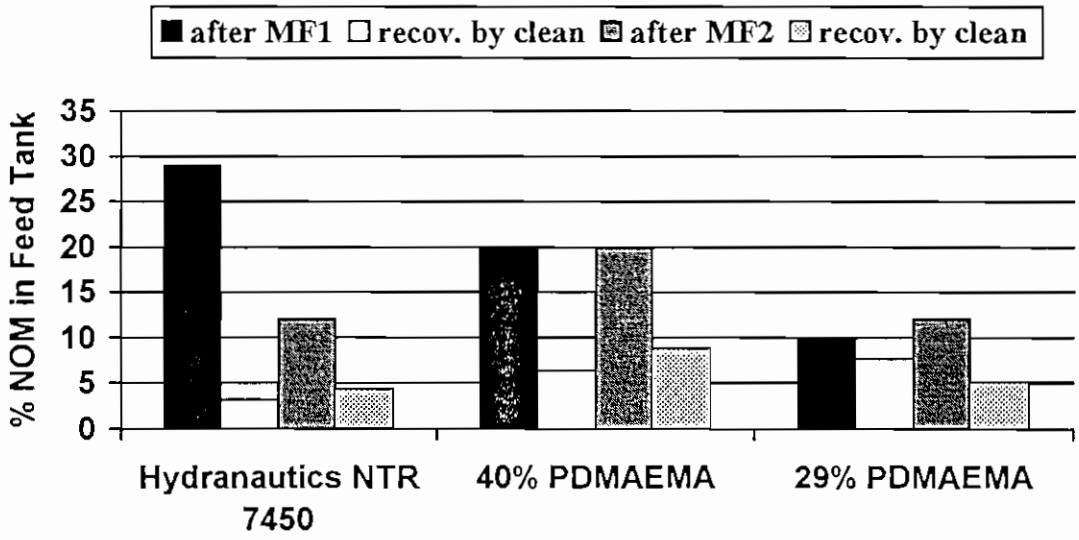

Figure 25. Efficiency of membrane cleaning for commercial and experimental membranes

SEMs also provided evidence for ineffective cleaning as well. The same "lacy" network structure for NOM was observed in SEMs after exposure of membranes to a NOM solution isolated from the Suwannee River by Braghetta, DiGiano and Ball[10]. Much of this structure remained after cleaning. In addition, there was evidence of microbial attachment.

Changes in Contact Angle and Surface Energies

Contact angle was measured with a VGA 2500 Video Camera (AST Products, Inc. Billerica, MA). In the *sessile drop* technique, the contact angle is that of a liquid drop on a solid surface that results from the cohesive forces inside the liquid drop and the solid surface and the adhesive forces between the solid and the liquid phases. The *captive bubble* technique is illustrated in Figure 26 wherein the membrane surface is submerged in water and the angle of the interface formed between an air bubble (θ_a) and the surface or between n-octane (θ_o), a non-polar liquid bubble, and the surface is computed with the aid of the video camera. The contact angle increases as the surface becomes more hydrophilic; this is opposite to the relationship in the sessile drop technique wherein the angle is measured between the water droplet and the surface, rather than the air or n-

octane bubble and the surface. Contact angles from both air and n-octane bubbles can be used to obtain fundamental relationship with surface-energy of the liquid and the solid, as well as the solid-liquid interfacial energy[19].

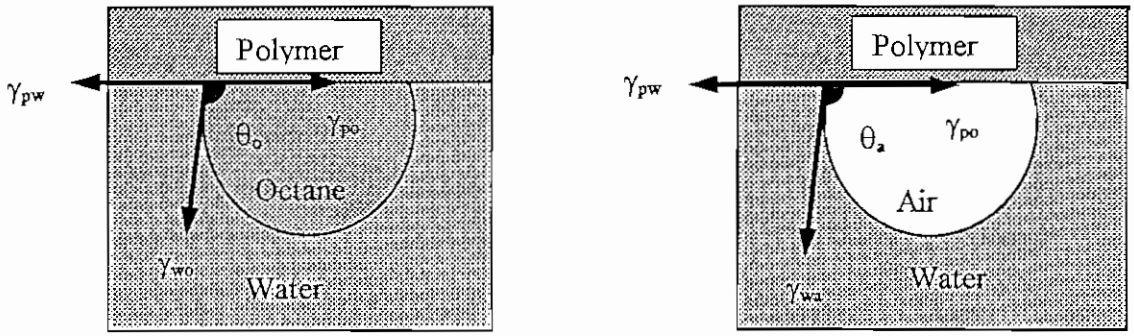

Figure 26. Schematic of Contact Angle Measurement in Captive Bubble Technique; γ = surface tension between two phases; p = polymer; w = water; o = n-octane; and a = air water

Contact angles were first determined for the dry surfaces of the three experimental membranes [PDMAEMA-b-FOMA (40 wt % PDMAEMA), PDMAEMA-b-FOMA (29 wt % PDMAEMA), and PFOMA], the commercial membrane (Hydranautics NTR 7450), and the polysulfone support layer. These measurements were repeated after contacting each of the surfaces for 20 min in EtOH and then submerging them into water as is usually done to open pores in the polysulfone support. With the exception of the PFOMA membrane, a NOM-containing solution of filtered-settled water from the P. O. Hoffer Water Treatment Plant was then filtered in dead-end mode with an Amicon test cell (about 4 cm in diameter) after which the contact angle was measured. The membranes were cleaned with the same cleaning solution (Zenon MC3) as used in the cross-flow tests and again, the contact angle was measured.

The results of contact angle measurements before after wetting of the membrane with ultrapure water (UPW) are listed in Table 10. A PFOMA membrane surface was included to provide a reference point for the most hydrophobic (exposure to a NOM containing solution was achieved in a static test because this membrane did not permeate water). As expected, the contact angles were the lowest for the PFOMA membrane.

Those for both PDMAEMA-PFOMA membranes were larger than for the PFOMA membrane but considerably smaller than for the Hydranautics NTR-7450 membrane or the polysulfone support layer. Thus, experimental membranes are more hydrophobic than the Hydranautics NTR-7450 membrane, the latter being a sulfonated polysulfone formulation. Wetting of the membranes somewhat decreased the contact angle implying that the surface became more hydrophilic.

The changes in contact angle upon exposure to a NOM containing solution and after cleaning are shown in Figure 27. Contact angle increased upon exposure to NOM for all but the Hydranautics NTR 7450 membrane. An increase in contact angle means that the surface becomes more hydrophilic.

Table 10. Contact angles (in degrees) for two vapor phases and different membrane materials

Membrane	Method	Dry	Wetted
Hydranautics NTR 7450	Air bubbles in the water	143	152
	n-octane bubbles in the water	114	100
PDMAEMA-b-FOMA (40 wt % PDMAEMA)	Air bubbles in the water	84	105
	n-octane bubbles in the water	64	92
PDMAEMA-b-PFOMA (29% wt% PDMAEMA)	Air bubbles in the water	72	91
	n-octane bubbles in the water	64	72
PFOMA	Air bubbles in the water	76	80
	n-octane bubbles in the water	27	19
Polysulfone	Air bubbles in the water	127	127
	n-octane bubbles in the water	70	71

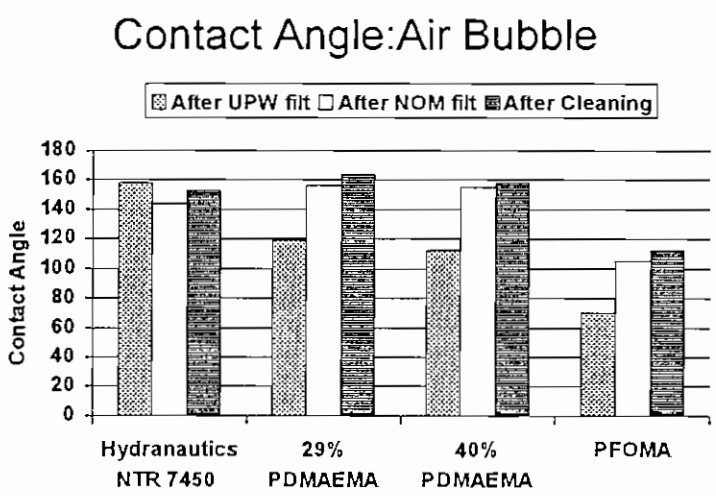

Figure 27. Changes in contact angle after exposure to a NOM containing solution and after chemical cleaning

The contact angles for the air and n-octanol bubbles (see Table 10) can be used to calculate dispersive and polar components of surface energy for the polymer in contact with its saturated vapor and the surface energy of the polymer-water interface. These calculated values are shown in Table 11. The sum of the dispersive and polar components of polymer-vapor surface energy is γ_{pv}. The PFOMA and the PDMAEMA-PFOMA experimental membranes have much lower γ_{pv} than the Hydranautics NTR 7450 membrane before contact with NOM. Their hydrophobic nature is also seen by the relatively high polymer-water surface energy (γ_{pw}) values. After contact with NOM, the γ_{pw} values were greatly reduced for PDMAEMA-PFOMA membranes. Thus, the interfacial surface energy between these relatively hydrophobic membranes and water became more hydrophilic. There was no decrease in γ_{pw} for the PFOMA membrane, probably because this surface was completely non- wetting and did not adsorb NOM.

Bouchard, et al.[20] found similar effects of NOM on membrane surface energy. A much greater decrease in interfacial energy (polymer-water) was found for a hydrophobic (cellulose acetate) than for a hydrophilic (polyamide thin film on polysulfone support)

Table 11. Calculated surface energies for membrane materials

Membrane	Component of Surface Tension[1]	Dry State (dyne/cm)	After Exposure to NOM and Chemical Cleaning (dyne/cm)
PFOMA	γ_{pv}^{p}	0.003	1.4
	γ_{pv}^{d}	25.3	80.0
	γ_{pv}	25.3	80.4
	γ_{pw}	50.2	53.2
29%PDMAEMA	γ_{pv}^{p}	3.6	44.6
	γ_{pv}^{d}	7.5	25.5
	γ_{pv}	11.1	70.1
	γ_{pw}	31.1	0.3
40% PDMAEMA	γ_{pv}^{p}	3.4	46.8
	γ_{pv}^{d}	18.4	20.6
	γ_{pv}	21.8	67.4
	γ_{pw}	28.1	0.1
Polysulfone	γ_{pv}^{p}	5.2	44.2
	γ_{pv}^{d}	82.3	25.6
	γ_{pv}	87.5	69.8
	γ_{pw}	42.8	0.4
Hydranautics	γ_{pv}^{p}	25.1	37.5
	γ_{pv}^{d}	41.1	28.6
	γ_{pv}	66.2	66.2
	γ_{pw}	7.5	1.5

[1] Definitions

γ_{pv}^{p} = polar component of polymer-vapor surface energy

γ_{pv}^{d} = dispersive (non polar) component of polymer-vapor surface energy

γ_{pv} = total polymer-vapor surface free energy

γ_{pw} = polymer-water interfacial energy decreased and the membrane surface

membrane. They calculated negative interfacial energies between polymer and water (about –30 dyne/cm) after NOM exposure and postulated that the NOM layer on the membrane was highly hydrated. They observed that negative interfacial energies are

common in biological and other aqueous systems, especially those characterized by strong monopolarity. Such interfaces are considered thermodynamically unstable and may rearrange to bring the surface energy back to 0 dyne/cm. They also noted from the literature that the greater the decrease in interfacial energy, the greater is the fouling potential. Hence, in their study, the cellulose acetate membrane had greater fouling potential than polyamide thin film composite membrane. Based on this same criterion, we would conclude that the PDMAEMA-PFOMA experimental membranes had a greater fouling potential than the Hydranautics NTR 7450 membrane.

The main observations can be summarized as:

1. Interfacial energy of the dry Hydranautics NTR-7450 membrane was less than for both PDMAEMA-PFOMA membranes, indicative of a more hydrophilic surface.
2. Interfacial energy did not change upon wetting of the Hydranautics NTR 7450 membrane and the polysulfone support layer but decreased for both PDMAEMA-PFOMA membranes (with greater change for the higher PDMAEMA weight percent). The surface of the PDMAEMA-PFOMA membrane could have reorganized itself upon wetting so that the PDMAEMA hydrophilic segments were in contact with the water.
3. Interfacial energy decreased very little for the Hydranautics NTR-7450 membrane upon exposure to NOM but decreased substantially more for both PDMAEMA-PFOMA membranes and for the polysulfone. The presence of hydrophobic PFOMA could be responsible for interaction with NOM that is more substantial than for the hydrophilic surface of the Hydranautics NTR 7450 membrane, sulfonated, polysulfone formulation.
4. Cleaning produced little change in interfacial surface energy for both the commercial and experimental membranes which adds further evidence to SEM results as to the ineffectiveness of the commercial cleaner used in this study.

Conclusions

Diblock and triblock copolymers of PDMAEMA and PFOMA were synthesized successfully by the iniferter technique. Much information was gained about the potential

of these materials for production of nanofiltration membranes through characterization of their dense film properties. TEM verified microphase segregation. The relationship of water flux to water uptake revealed the importance of selecting the hydrophilic block (PDMAEMA) content to achieve a membrane material that would be comparable to commercial products. NaCl and NOM partitioning and NaCl diffusion measurements also revealed the importance of copolymer composition to estimate solute rejection and possibly fouling potential.

Whether diblock copolymers synthesized from a hydrophobic and hydrophilic polymer offer an advantage over commercially available membrane materials remains to be proven. These first two experimental membranes showed that water flux-pressure was comparable to a commercial membrane. It may be possible to prepare other block copolymer formulations with higher flux. The relatively poor rejection of NOM for these experimental membranes may have been due to hydrolysis of the block copolymer during cleaning at pH. 10.3. Either structural modifications or a change in cleaning method may solve this problem. Unfortunately, these experimental membranes were also subject to as much fouling as the commercial membrane.

In this early work, it was clear that once the surface is fouled, the contact angle (and thus the surface energy) did not return to that of clean membrane surface. Irreversible fouling is suggested but the implication for recovery of water flux after repeated cleanings is not clear. Repeated cycles of flux decline and cleaning would be needed to determine the long-term change in surface energy and whether alternative cleaning techniques may be more effective.

Although these early results were not encouraging, an experimental approach has been described which can lead to a better understanding of the relationship between physical-chemical properties of polymers and their membrane filtration characteristics. Other polymer formulations (e.g., different hydrophobic and hydrophilic block combinations; different molecular weights of each block; triblock vs. diblock copolymers and addition of cross-linking) can be investigated.

Casting and testing of thin-film composite membranes requires considerable time. A more fruitful approach is to focus on the properties of dense films as was demonstrated

in this work. Once a particular dense film formulation shows promise, thin-film membranes can be formed for more practical tests.

References

1. A. Pittman. 1972. Surface Properties of Fluorocarbon Polymers. in Fluoropolymers ed. by Leo A. Wall, Chapt. 13
2. R. Ramharack and T. H. Nguyen. 1987. *J. Polym. Sci.*, 25C: 93
3. W. Noll. 1968. Chemistry and Technology of Silicones, Academic Press, New York
4. J. M. DeSimone, Z. Guan and C. S. Elsbernd. 1992. *Science*, 257:945
5. Z. Guan, C. S. Elsbernd and J. M. DeSimone. 1992. *Polym. Prep. (Am. Chem. Soc. Div. Polym. Chem.)*, 33:329
6. Z. Guan and J. M. DeSimone. 1992. *Polym. Prep. (Am. Chem. Soc. Div. Polym. Chem.)*, **33**:172
7. Z. Guan and J. M. DeSimone. 1994. *Macromolecules*, **27**:5527-5532
8. Z. Guan, J. R. Combes, C. S. Elsbernd and J. M. DeSimone. 1993. *Polym. Prep. (Am. Chem. Soc. Div. Polym. Chem.)*, **34**:447
9. Braghetta, A., F. A. DiGiano, W. P. Ball. 1997. *Jour. Environ. Engrg., ASCE*, **123**:628-641
10. Braghetta, A., F. A. DiGiano, and W. P. Ball. 1998. *Jour. Environ. Engrg., ASCE*, **124**:1087-1098
11. M. K. Bernett and W. A. Zisman, 1962. *J. Phys. Chem.*, **66**:1207
12. Betts, D. E., T. Johnson, D. Leroux, and J. M. DeSimone. 1998. ACS Symposium Series 685, Chapt. 25, 418-432.
13. D. J. Meier. 1969. J. Polym. Sci. 26C, 81
14. J. Brandrup, E.H. Immergut, Polymer Handbook 3rd Edition, John Wiley & Sons
15. Lonsdale, H. K, B. P. Cross, F. M. Graber, and C. E. Milstead. 1971. *Jour. Macromol.-Phys.* **B5(1)**: 167
16. Jucker, C. and M. M. Clark. 1994. *Jour. Membrane Sci.* **97**:37
17. Clark, M. M. and P. Lucas. 1998. *Jour. Membrane Sci.* **143**:13
18. DiGiano, F. A., S. Arweiler, and J. A. Riddick. 1998. Proceedings of *AWWA Annual Conference*, Dallas, TX (pp. 35-60)
19. Andrade, J. D., S. M. Ma, R. N. King and D. E. Gregonis. 1979. *Jour. Colloid and Interface Sci.* **72**:3:488
20. Bouchard, C. R., J. Jolicoeur, and P. Kouadio. 1997. *The Canadian Jour. of Chem. Eng.*, **75**:339